SANDIA REPORT

SAND2001–8444
Unlimited Release
Printed August 2001

Micro-fabricated Solid State Neutron Generators

J.C. Lund, J.M. Van Scyoc, N.R. Hilton, K.L. Hertz, A.M. Morales, and G. Hux

Prepared by
Sandia National Laboratories
Livermore, California 94550

Sandia is a multiprogram laboratory operated by Sandia Corporation, a Lockheed Martin Company, for the United States Department of Energy under Contract DE-AC04-94AL85000.

Issued by Sandia National Laboratories, operated for the United States Department of Energy by Sandia Corporation.

Available to DOE and DOE contractors from
Office of Scientific and Technical Information
P.O. Box 62
Oak Ridge, TN 37831

Prices available from (615) 576-8401, FTS 626-8401

Available to the public from
National Technical Information Service
U.S. Department of Commerce
5285 Port Royal Rd
Springfield, VA 22161

NTIS price codes
Printed copy: A11
Microfiche copy: A01

SAND2001-8444
Unlimited Release
Printed August 2001

Micro-fabricated Solid State Neutron Generators

J.C. Lund, J.M. Van Scyoc, N.R. Hilton, K.L. Hertz, A.M. Morales and G. Hux
Sandia National Laboratories
P.O. Box 969
Livermore, CA 94551-0969

Abstract

The traditional neutron generators used in nuclear weapons systems, and in many industrial gauging applications, employ a portable ion accelerator with tritium target. Such neutron "tubes" work well, but they are difficult to make in small sizes, require high voltage power systems, and have a limited shelf life. Another approach to neutron generation involves the use of an alpha-emitting radioisotope mixed with beryllium. The traditional disadvantage of such an alpha-Be source is that they are always "on"; that is, they emit neutrons at a steady rate even when stored. Thus, it is extremely awkward to use a conventional alpha-Be source in many applications because of the neutron shielding required to prevent exposure to personnel and sensitive electronics. However, with the advent of modern micro-machining techniques it is possible to build a "switchable" all solid state neutron source. This report describes our research into demonstrating the feasibility of such micro-machined Solid State Neutron Generators (SSNGs). Our research indicates that it is not feasible to employ this technology in a nuclear weapon application. However, these SSNGs show great promise for industrial and treaty monitoring applications.

Intentionally Left Blank

Contents

Preface

This report describes research performed for an LDRD project titled "Solid State Neutron Generators for use in Nuclear Weapons" (LDRD project #10351). The title of this report differs from the title of the LDRD research program because- it was thought by the authors- the report would be of interest to a wider audience than the original LDRD title would suggest. The title change is also more closely aligned with the conclusion of the research described in this report; the research showed that switchable Solid State Neutron Generator (SSNGs) are not an appropriate technology for use in Nuclear Weapons. However, the research indicated that the devices described in this report might be very useful in other, non-weapon, applications.

The report is divided into the following sections:

- **Section 1** consists of an introduction and background on the topic of solid state neutron generators so that the reader may understand more clearly the implications of the research described in subsequent chapters.

- **Section 2** details our research into finding the most appropriate alpha-emitting radioisotope for use in a SSNG. A detailed examination of alpha emitters was necessary because their properties determine – to a very large degree- the applicability of the neutron generator, as well as many of the design characteristics of SSNGs.

- **Section 3** describes a detailed quantitative theory of the operation of a solid state neutron generator, which was developed as part of the research project.

- **Section 4** describes the experiments that were performed to determine the feasibility of solid state neutron generators as well as to validate the quantitative theory outlined in the previous section. This section also describes our successful development of micro-fabrication processes for SSNGs production.

- **Appendix A**

The appendix lists the references to literature specifically cited, as well as those generally used in the preparation of this report.

Executive Summary

This report describes a two-year research and development program aimed at investigating a new type of neutron generator for possible use in nuclear weapons. The new devices we investigated, Solid State Neutron Generators (SSNGs), are constructed using micro-fabrication methods and rely on the reaction of alpha particles from a radioisotope with a beryllium foil. Unlike traditional alpha particle –beryllium generators, the new devices we investigated can be switched on and off (through micro-machine action).

We determined from our research that the SSNGs we investigated would not be a very good choice for use in nuclear weapons. However, our research did uncover some surprising behavior from these new devices. These largely unanticipated properties would seem to make them very attractive for other (non-nuclear-weapon) applications. In particular, we discovered that it is possible to build small neutron generators with anisotropic emission properties- neutron flashlights if you will. The anisotropic generators could be very useful in treaty monitoring applications and perhaps even in industrial gauging and imaging applications. We are very interested in further investigating this technology for these new applications.

We arrived at our conclusions about the utility of these new generator devices by investigating several aspects of their behavior. Our research was roughly divided in to four areas: 1. the search for appropriate radioisotopes to drive the generator, 2. development of quantitative methods to predict generator performance, 3. experimental validation of the quantitative methods, and 4. investigation of methods to fabricate micro-machined neutron generators.

Our search for alpha particle emitting radioisotopes consisted of a systematic investigation of all isotopes that emitted alpha particles with a (parent) half-life of between 1 and 100 years. We found eighteen radioactive alpha emitting isotopes that satisfied this criteria and we investigated each one of them for two characteristics: 1. their ultimate efficiency with which they could generate neutrons in a solid state generator (a desirable property), and 2. the dose that they would produce by collateral emission of gamma-rays (an undesirable property). We then analyzed the tradeoff between desirable and undesirable characteristics for all isotopes and found that one isotope, 238Pu, was the single optimal isotope to use in a solid state neutron generator.

Another major effort of our research program was the development of a quantitative model to estimate the performance characteristics of a neutron generator before actually building one. Clearly a trial-and-error development effort for these new devices was out of the question, given the immense administrative challenges in performing trial experiments with exotic radioisotopes and the danger of generating “mixed waste” (debris containing radioactive products and toxic beryllium). In fact, at the site where the project was conducted- SNL/CA- it is specifically forbidden to generate mixed waste of any quantity. These administrative constraints had a strong influence on the strategy we developed to execute the research program, and placed an unanticipated additional emphasis on predictive

computation techniques. Thus, after searching unsuccessfully for previously developed computer models of alpha-Be generator performance, we developed our own computation tools for predicting the characteristics of these new devices. Our computation technique involved the creation of a 3-dimensional analog Monte-Carlo computer program to model the transport of alpha particles in the micro-devices. The output of the alpha transport code was then coupled to another computer program, which predicted the distribution of neutrons produced in an energy-angle phase space. Our quantitative methods were later validated by experimental results. In addition to serving the utilitarian role of predicting device performance, the computer codes allowed us to visualize the neutron generation characteristics, and- in so doing- envision new applications for them.

Concurrent with our computation efforts, we conducted an experimental program to measure the neutron output from specific isotope-beryllium pairings. We eventually constructed experiments which measured both the total neutron output and angular distribution of 241Am and 225Ac emitters impinging on beryllium targets. These experiments took considerable resources to conduct. Great care had to be exercised in obtaining the administrative approval to conduct these experiments. The experiments themselves were physically very large (owing to shielding requirements) and mechanically and electronically complex; in short, they were a major challenge to our experimental technique.

The final topic that we investigated in this research program was the feasibility of fabricating micro-parts for use in SSNGs. This phase of the research program was conducted successfully, and we were able to fabricate parts with the requisite dimensions in suitable patterns and from dense materials (gold).

In summary, the research program described in this report was a successful one. We were disappointed when we discovered that our devices would not work in their intended application (nuclear weapons). However, we were pleased to discover that these devices had other characteristics (most notably, anisotropic neutron emission) which would allow them to be used in new applications.

Section 1. Background

Conventional Neutron Generators

Nuclear weapons in the current inventory make use of neutron generators in the firing system. Existing neutron generators are constructed using a vacuum tube technology. In particular, the neutron generators designed by Sandia and used in existing weapons make use of the deuterium-tritium (D-T) reaction. Deuterium ions are accelerated in an electrostatic potential in high vacuum at a target (usually a metal hydride) containing tritium. While D-T neutron generators have served well, they posses a number of disadvantages in terms of reliability, longevity and difficulty of manufacture. Because existing neutron generators make use of vacuum technology, great care must be used in their manufacture to insure that the electrical and mechanical seals are robust, and not prone to failure with aging. Even if a conventional neutron tube could be manufactured with perfect reliability, the useful lifetime of the tube is limited by the half-life of the tritium in the target. The tritium used in the target material has a half-life of 12 years; thus after 25 years, the neutron yield from the generator would be diminished by about a factor of five. Great care must also be exercised in the design and manufacture of neutron generators to insure that they are capable of handling the extreme physical and mechanical environments a weapon might be exposed to.

Alpha-Beryllium Neutron Generators

To mitigate the problems inherent in existing neutron generators, we set about to examine the feasibility of a new design and manufacturing process for neutron generators. The design we investigated was an all solid state one and does not make use of vacuum tube technology. The new type of neutron generator that we investigated produces neutrons from the reaction of energetic alpha particles with beryllium nuclei.

The alpha-beryllium reaction has been used for many years as a method for producing neutrons. However, existing alpha-beryllium sources are manufactured by alloying beryllium with an alpha-emitting isotope such as ^{241}Am or ^{240}Pu. A diagrammatic view of the operation of a conventional alpha-beryllium generator is shown in **Figure 1-1**. Thus, conventional alpha-Be sources continuously emit neutrons and could represent a significant health risk to anybody in the vicinity of their use.

Switchable Alpha-Beryllium Neutron Generators

In this research program, we investigated a “switchable” alpha-beryllium neutron source that, if properly designed, would emit a negligible number of neutrons or other types of radiation when in the “off-state”. The new neutron generator design consisted of a layer of an alpha emitting radioactive source separated from a layer of beryllium metal by a movable micro-machined layer. A diagrammatic view of the operation of a switchable solid state generator is shown in **Figure 1-2**.

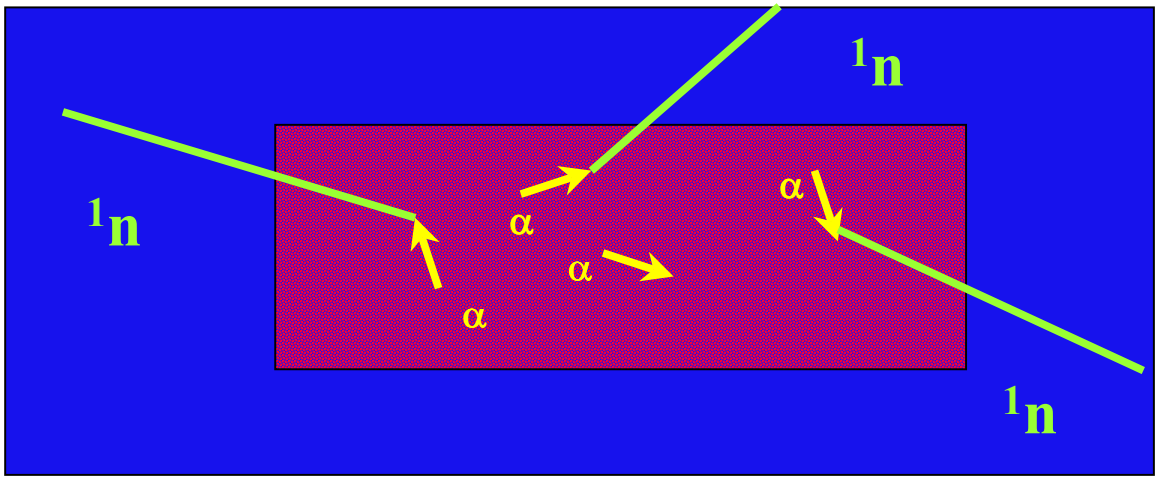

Figure 1-1. Diagrammatic illustration of the operation of a typical alpha-Be neutron source. The source is formed by alloying an alpha-emitting radioisotope with beryllium. The alpha particles have a short range in the beryllium (less than 1 mm), the neutrons, however, travel freely out of the device once they are produced.

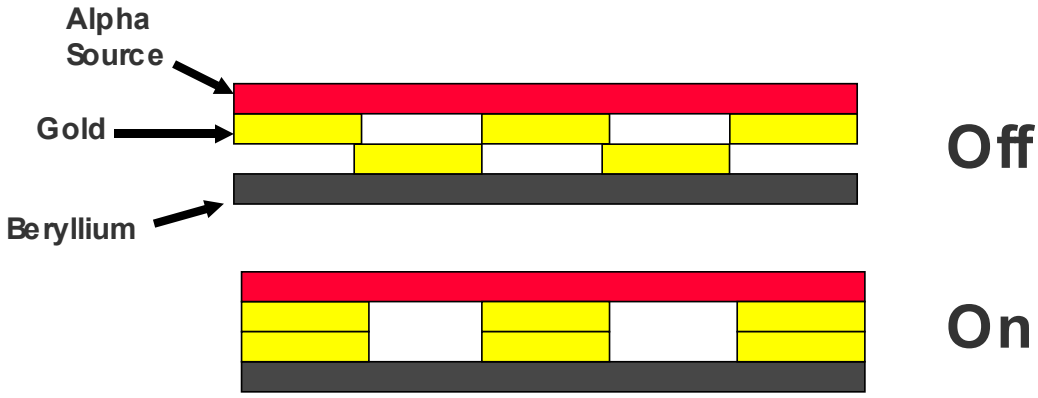

Figure 1-2. Diagrammatic illustration of the operation of a micro-machined, switchable, solid state neutron generator. The upper diagram illustrates the device in the off-state, where a thin layer of gold is blocking the passage of alpha particles from the source to the beryllium absorber. By shifting the phase of the plates with respect to each other, the device can be switched on (lower diagram). This particular design of switched SSNG became known as the pumpkin-teeth design, owing to the topology of the gold absorbers in the off state.

Section 2. Candidate Alpha Particle Emitting Isotopes

Introduction

The properties of the alpha emitting source that is used in a potential solid state neutron generator, will determine the utility of the generator in any given application. In particular, the properties of the alpha-emitting isotope will ultimately determine the maximum neutron emission rate, as well as the dose due to collateral radiation that is produced by the generator in the off-state. With our present technology and understanding of nuclear physics, it is not possible to produce new isotopes with tailored properties for our application (nor is it likely that it ever will be possible). Instead, we are forced to choose from the palette of existing radioactive isotopes. Fortunately the palette is a fairly large one, and in this section of the report we will detail our exploration of the Table of the Isotopes (the list of all existing nuclei) in search of optimal radioisotopes for neutron generators. It is worth noting that much of this search required painstaking examination of large quantities of compiled experimental data on isotopic properties. Because atomic nuclei are very complex entities (composed of many particles with multiple complex forces operating on these particles), it is extremely difficult to predict the properties of a given nucleus based on first principles. Instead it is necessary to apply a few general rules, and then pore through the experimental data for any given isotope and compute its desirability based on previously measured properties. Fortunately, combing though this vast quantity of experimental data has become somewhat less painful in recent years with the advent of Internet searchable databases of nuclear properties; extensive use of these new search tools was used during the course of the research project.

In this section of the report we will first discuss the properties of a radioisotope that make it desirable or undesirable for use in a neutron generator. The first property we will examine is the ultimate neutron production efficiency that a radioisotope could achieve when used in a neutron generator. Once we have developed some quantitative methods for predicting the neutron production rate we move to the next sub-section in which we enumerate the list of possible alpha emitting isotopes. With our list of possible candidates in hand, we then examine the detailed systematics of the decay chain of each candidate isotope. This examination will then yield the emission properties of collateral particles (gamma-rays) and thus allow us to compute the dose to human beings from each candidate isotope. With a knowledge of the good (neutron production rate) and the bad (gamma-ray dose rate) we will conclude this section with a subsection on the evaluation of tradeoffs between good and bad and the selection of an optimal isotope for a particular neutron generator application.

Efficiency of Alpha Emitting Sources

An obviously essential requirement of an alpha-emitting isotope in an alpha-Be generator is that the generator produces neutrons—ideally as many neutrons as possible.

The efficiency of alpha-Be sources has been studied by a number of groups over the years. Geiger and Van der Zwan [Geiger 75] reviewed the literature in 1975 and developed the following empirical relationship between the energy of the emitted alpha particle and its efficiency for producing neutrons in a thick (greater than the range of the alpha particle) Be target:

$$Y(E) = 0.95 \times 0.152 E_{\alpha}^{3.65} \tag{2.1}$$

where E_{α} is the energy of the alpha particle in MeV and $Y(E)$ is the efficiency of neutron production (in units of neutrons per 10^6 alpha particles impinging on the Be target). Equation (2.1) tells us that there is an extremely strong dependence of neutron production rate on increasing alpha particle energy; a plot of this relationship is show in **Figure 2-1**. Of course, as neutron generator designers, we are interested in the absolute neutron generation rate, not the efficiency per alpha particle. To get the absolute rate of neutron production we must compute the rate of alpha emission from the source. The rate of alpha production from a source depends on the half-life of the source and the branching ratio for alpha particle production versus competing nuclear decay processes such as beta decay or spontaneous fission. To relate the alpha emission rate to the size of the generator we can use the specific activity (*SA*) or emission rate per unit mass of source.

$$SA_{\alpha} = \frac{0.69 N_A BR}{t_{1/2} M} \tag{2.2}$$

where N_A is Avogadros number (6.022×10^{23} $atoms/mole$), *BR* is the branching ratio for alpha emission of a particular energy, $t_{1/2}$ is the half-life, and *M* is the atomic weight (in grams/mole) of the emitting isotope.

Equations (2.1) and (2.2) can be multiplied together to give the neutron production rate per gram of alpha particle emitter for any alpha particle emitted by an isotope. This process can then be repeated and summed for each alpha particle emission energy emitted by the isotope under consideration to obtain the total neutron emission rate Y_{total}

$$Y_{total} = \sum_i SA_{\alpha i} Y(E_i) \tag{2.3}$$

where $SA_{\alpha i}$ is the specific activity for the i^{th} alpha emission of energy E_i.

Figure 2-2 illustrates the relationship between neutron production rate and mass for three hypothetical alpha emitters which emit just one alpha particle energy (with a 100% branching ratio for that transition). Examination of **Figure 2-2** indicates that, in principle at least, quite prodigious neutron production from a small solid state generator could be achieved if the right isotope were found. However, one of our colleagues pointed out [James 00] that the total neutron production rate would be limited by power dissipation in the generator. Since only a negligible fraction of the alpha particle energy is carried away by neutrons, to first order the power generated in a solid state neutron generator is given by the alpha production rate. For instance, one gram of a hypothetical 6 MeV alpha emitter with a half-life of 6 years would produce about 10^9 neutrons per second, but would dissipate 9.6 W of thermal power in a close proximity to the alpha emitting layer. As we will see later in this

section, other factors (notably gamma-ray production rate) might also constrain the maximum attainable neutron production rate.

Possible Alpha Emitting Sources

In the previous sub-section we saw that there were two main factors that were a necessary condition for an alpha particle source used in a solid state neutron generator. In this sub-section we will use these criteria to select a few alpha-emitting isotopes for further detailed study.

A portion of the Table of the Isotopes (a Nuclear Physicist's analog to a Chemist's periodic table) is shown in Figure 2-3. There are a few hundred possible isotopes to choose from. Based on half-life alone, though, we can eliminate a great many of the alpha-emitting isotopes. If we assume that we would like our hypothetical neutron generator to have a reasonable useful life we can constrain the half-life to be greater than 1year. Conversely, if we want our hypothetical generator to be somewhat small and efficient we should constrain the half-life to be less than 100 years. The bounding of the half-life of between 1 and 100 years drastically reduces the number of isotopes under consideration to eighteen. The 18 candidate alpha emitting isotopes are listed in Table 2-1.

Systematics of Candidate Isotope Decay

Before we can determine which of the eighteen isotopes listed in Table 2.1 might produce the best performing neutron generators we must perform a rather detailed study of the decay characteristics of each of these candidate isotopes. Unfortunately, because all of the candidate isotopes are heavy, complex nuclei they tend to decay in complex sequences before finally arriving at a stable long-lived configuration. Examining the decay characteristics of each candidate isotope is important for two reasons: 1. We must tally up all of the alpha particles emitted in the decay scheme to compute the estimated efficiency for creating neutrons, and 2. We must tally all of the collateral emissions (particularly gamma-rays) so we can estimate the dose from a generator when it is in the off state.

Figures 2-4 through Figure 2-21 detail, in diagrammatic fashion, the decay chain of each of the eighteen isotopes listed in Table 2.1. In perusing the decay sequences we note that several of the decay sequences (e.g. ^{232}U in Figure 2-11) produce daughter nuclei who themselves decay with half-life comparable to the parent nucleus. Under these conditions (when the daughters decay not too fast) we would expect the output of a neutron generator made from such an isotope to vary with time (it could increase or decrease in intensity with time). In other words, as the parent nucleus equilibrates with its daughters the relative emission intensity of alpha particles will change as the daughter population increases.

Dose from Alpha Emitting Sources

In addition to allowing us to compute the potential efficiency of an isotope in a neutron generator, our examination of the decay sequence also allows us to compute the dose rate produced from collateral gamma-rays produced in the decay sequence. Unfortunately, most of the nuclei in our candidate list do not simply undergo alpha decay to the ground state of the daughter nucleus, instead they often decay to an excited daughter state which will

subsequently decay to the ground state via gamma-ray photon emission. Or, the daughter may decay by some other mode (beta decay or electron capture) but again to an excited state which subsequently produces a gamma-ray. We analyzed the decay sequence of all 18 candidate emitters and computed the emission probabilities of gamma-rays for all decay chains as a function of time. An example of the computed gamma-emission probabilities for a given decay sequence is shown in Figure 2-23, where the emission probabilities for 225Ac decay are shown.

Once the emission probabilities of gamma-rays for a given decay sequence were calculated we could then estimate the dose, or more accurately the RBE or relative biological dose equivalent. The RBE for gamma-rays was computed by multiplying the vector of gamma-ray emission probabilities for a given isotope with the vector of values relating dose to gamma energy recommended by the standards organizations [ANSI 91]. The dose energy relationship for gamma-rays we used in our calculations is plotted in Figure 2-22. The result of a dose calculation for 225Ac is shown in Figure 2-24, normalized to the emission rate of the source, and- in Figure 2-25- normalized to the mass of the emitting isotope. We performed our dose calculations under at least two conditions: a bare source, and the source with some small amount of shielding. Nominal shielding was included in the calculations because, in any application, the source is likely to be surrounded by some materials. We wanted to avoid the possibility of eliminating a candidate isotope because its dose rate was too high, if the dominant dose was due to low energy gamma-rays (which can be easy to shield).

Selection of Optimum Alpha Emitting Isotope

With our calculations of the estimated neutron production rate and gamma dose rate complete, we were in a position to estimate the trade-off between neutron production rate and gamma-ray dose for all of the candidate isotopes. The results of this tradeoff are plotted in **Figure 2-26** for a 10-year-old source and in **Figure 2-27** for freshly produced source 30 days old.

In our initial analysis of the data presented in **Figures 2-26** and **2-27** we could not resolve any optimal alpha emitting source for use in a SSNG. Depending on the application on which the generator is going to be used, we can, apparently, choose an isotope that is optimal. For instance, if minimizing the dose rate in the off-state is the primary consideration ^{238}Pu is clearly the best choice. If, on the other hand, we wish to maximize the neutron production rate (at a moderate dose) ^{227}Ac and ^{232}U appear to be good choices.

However, one of the authors of this report (Hilton), suggested an alternative method to analyze the data presented in **Figures 2-26** and **2-27**. This alternative analysis method normalizes the gamma-ray dose to the neutron production rate. In this interpretation, shown graphically in **Figures 2-28** and **2-29,** we are computing the penalty incurred (gamma-ray dose) per gain (neutron produced). Using this optimization strategy ^{238}Pu is the clear winner (provided some nominal shielding is used).

Summary

An important consideration in the design of a solid state neutron generator is the selection of the radioactive isotope that emits alpha particles in the generator (which subsequently produce neutrons). We examined a subset of all alpha-emitting isotopes (those with a half-life between 1 and 100 years) and found eighteen that were potential candidates for use in SSNGs. More detailed examination of each of these isotopes and the application of an optimization strategy indicated that one isotope was superior. This isotope, ^{238}Pu, was the best when an optimization strategy which minimized the gamma-ray dose (undesirable feature) per neutron production rate (most desirable feature) was applied to the list of candidate isotopes.

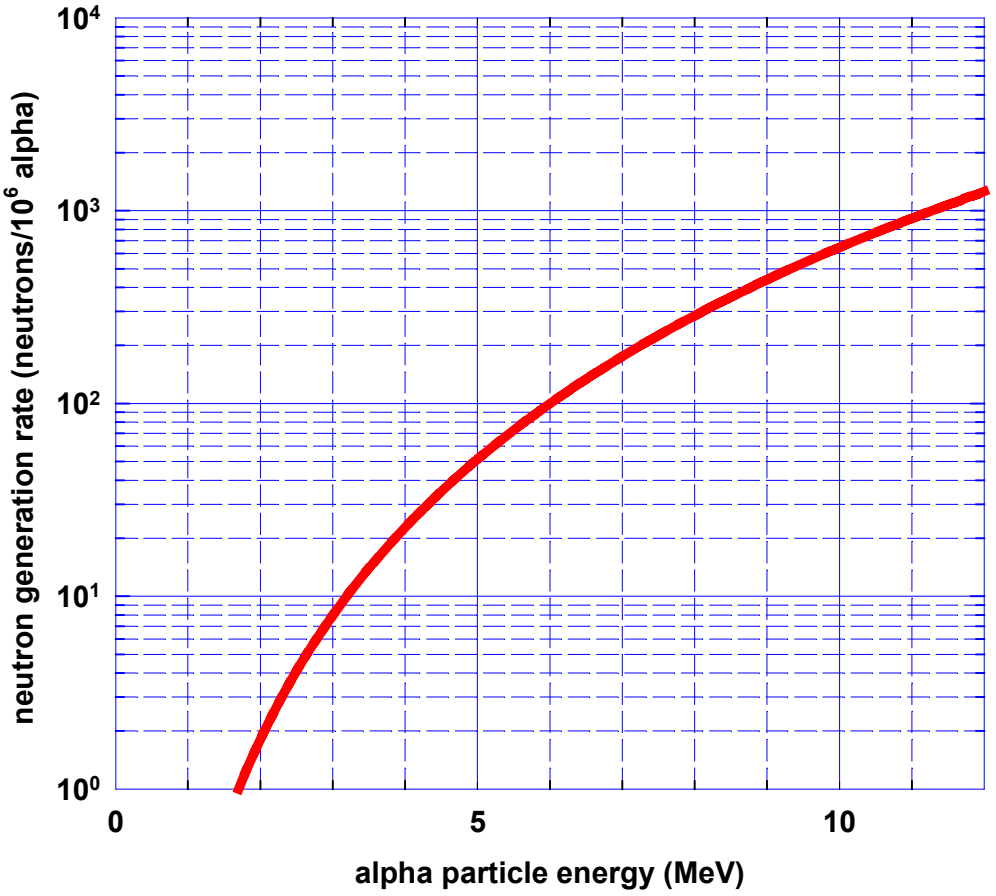

Figure 2-1. Neutron generation rate as a function of alpha particle energy. This is a plot of the empirical relation developed by Geiger and Van der Zwan [Geiger 75]. The graph indicates the number of neutrons that would be produced when a mono-energetic alpha particle stops in a beryllium target thicker than the range of the alpha particle. Note the strong increase in neutron production as the energy of the impinging alpha particle increases.

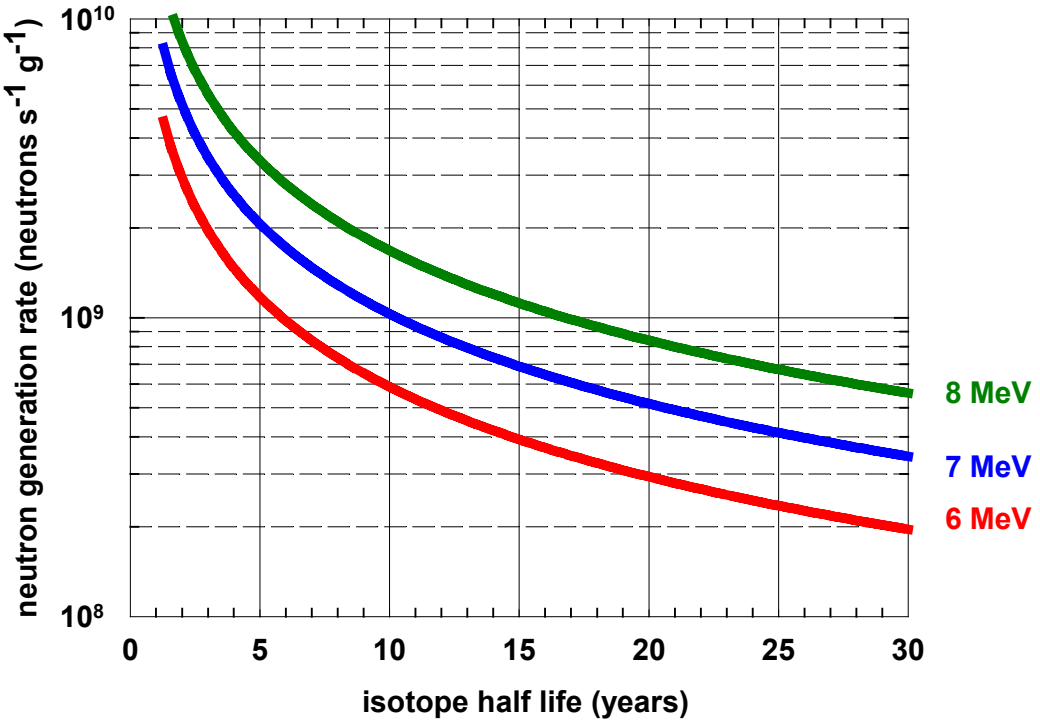

Figure 2-2. Neutron generation rate as a function of alpha emitter half-life for three alpha particle energies. Because the specific activity (emission rate per mass of material) increases as the half-life decreases, shorter half-life alpha sources produce alpha particles (and hence neutrons in a alpha-Be generator) at a greater rate than longer half-life emitters. A short half-life is desirable because greater neutron production rates can be produced by smaller amounts of material. A short half-life is also desirable from an environmental perspective, as the material in the generator will "cool" faster and present less of a hazard over time. Of course, the drawback of a short half-life source is that the lifetime of the neutron generator is reduced, a factor of great significance in a nuclear weapon application.

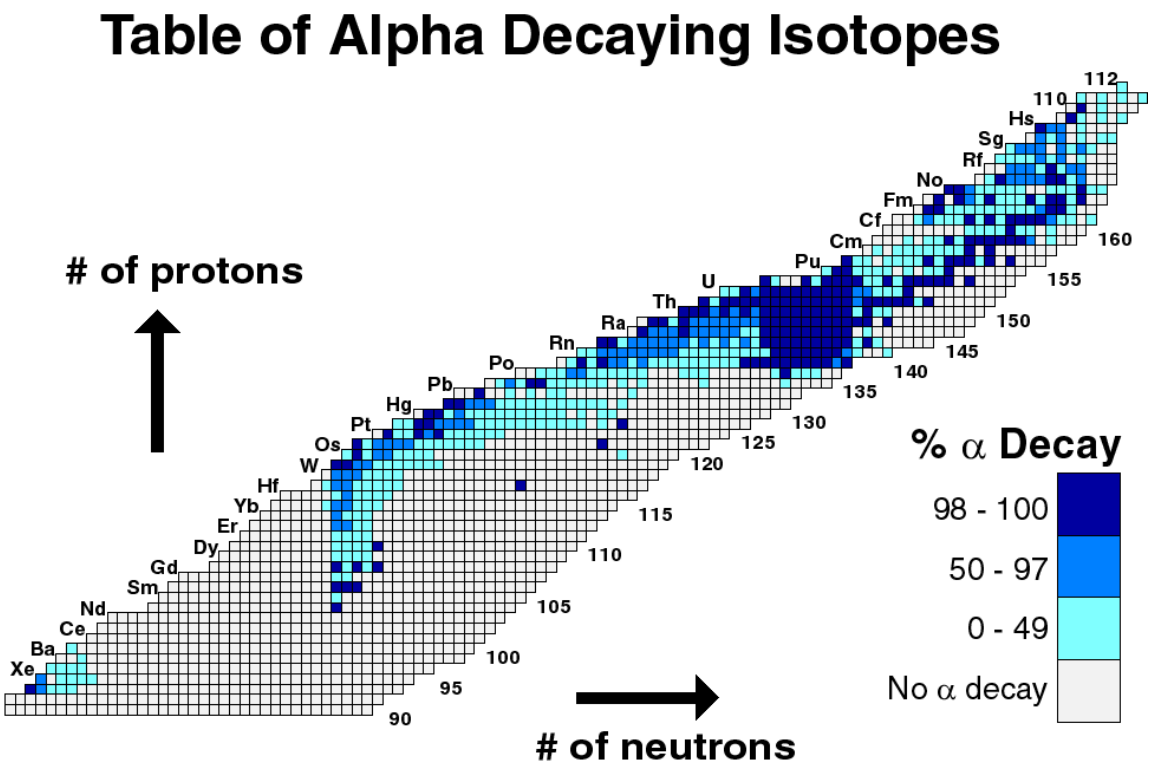

Figure 2-3. Portion of the Table of the Isotopes showing the occurrence of alpha emitting radioisotopes. In general alpha decay is more prevalent for nuclei with a large number of nucleons (neutrons and protons). In large nuclei, Coulomb repulsion begins to compete with the short-range nuclear forces and alpha decay becomes much more likely. Note too, that amongst high nucleon nuclei, proton rich nuclei are even more susceptible to alpha decay.

Nuclide	Half-life
^{145}Pm	17.1 y
^{148}Gd	74.6 y
^{208}Po	2.89 y
^{210}Pb	22.3 y
^{227}Ac	21.7 y
^{228}Ra	5.75 y
^{228}Th	1.91 y
^{232}U	68.9 y
^{235}Np	396. d
^{236}Pu	2.86 y
^{238}Pu	87.7 y
^{241}Pu	14.3 y
^{243}Cm	29.1 y
^{244}Cm	18.1 y
^{248}Bk	>9 y
^{250}Cf	13.1 y
^{252}Cf	2.65 y
^{252}Es	471. d

Table 2-1. Alpha particle emitting isotopes with a half-life of between 1 and 100 years. These isotopes comprised the main candidates for use in a long lasting neutron generator (such as would be used in a nuclear weapon) that were examined as part of this study.

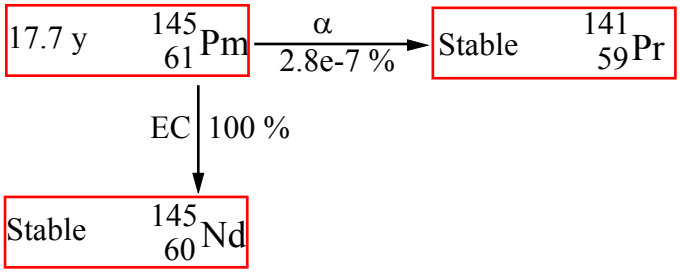

Figure 2-4. Decay chain diagram for ^{145}Pm. EC refers to an electron capture decay mode.

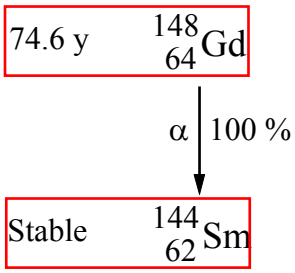

Figure 2-5. Decay chain diagram for ^{148}Gd.

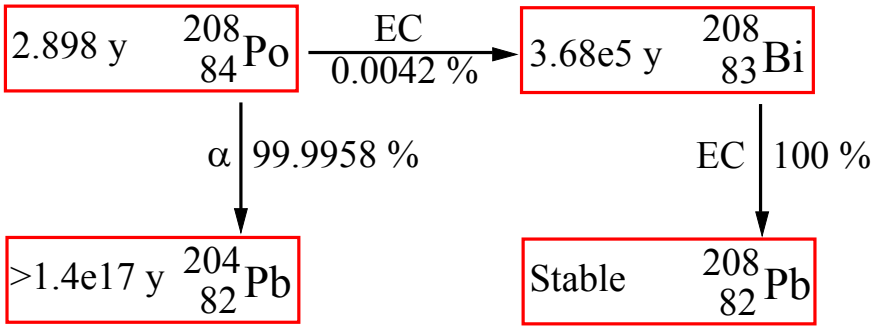

Figure 2-6. Decay chain diagram for ^{208}Po.

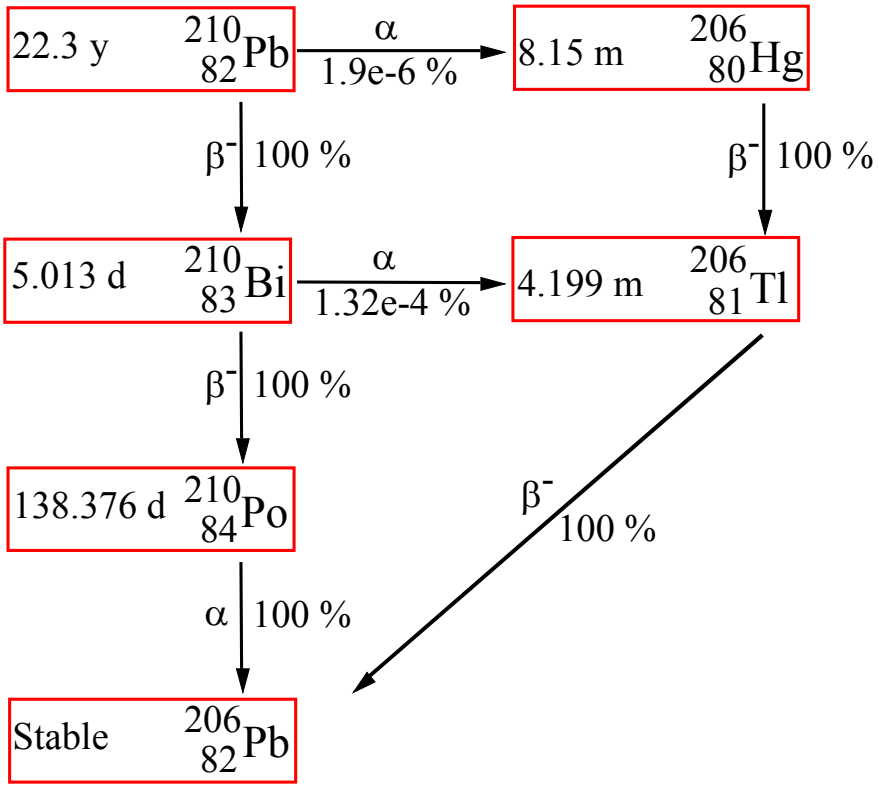

Figure 2-7. Decay chain diagram for ^{210}Pb.

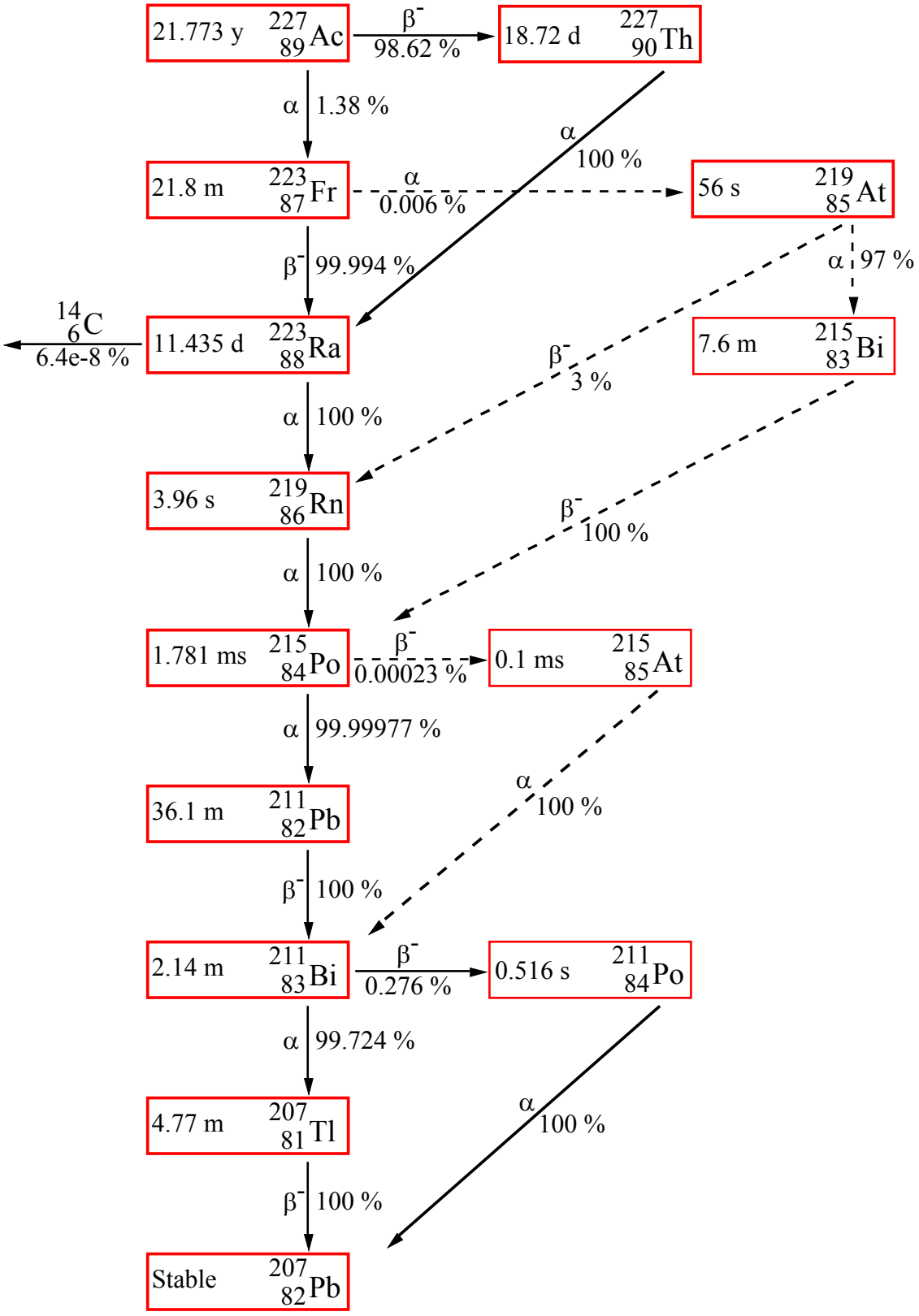

Figure 2-8. Decay chain diagram for ^{227}Ac

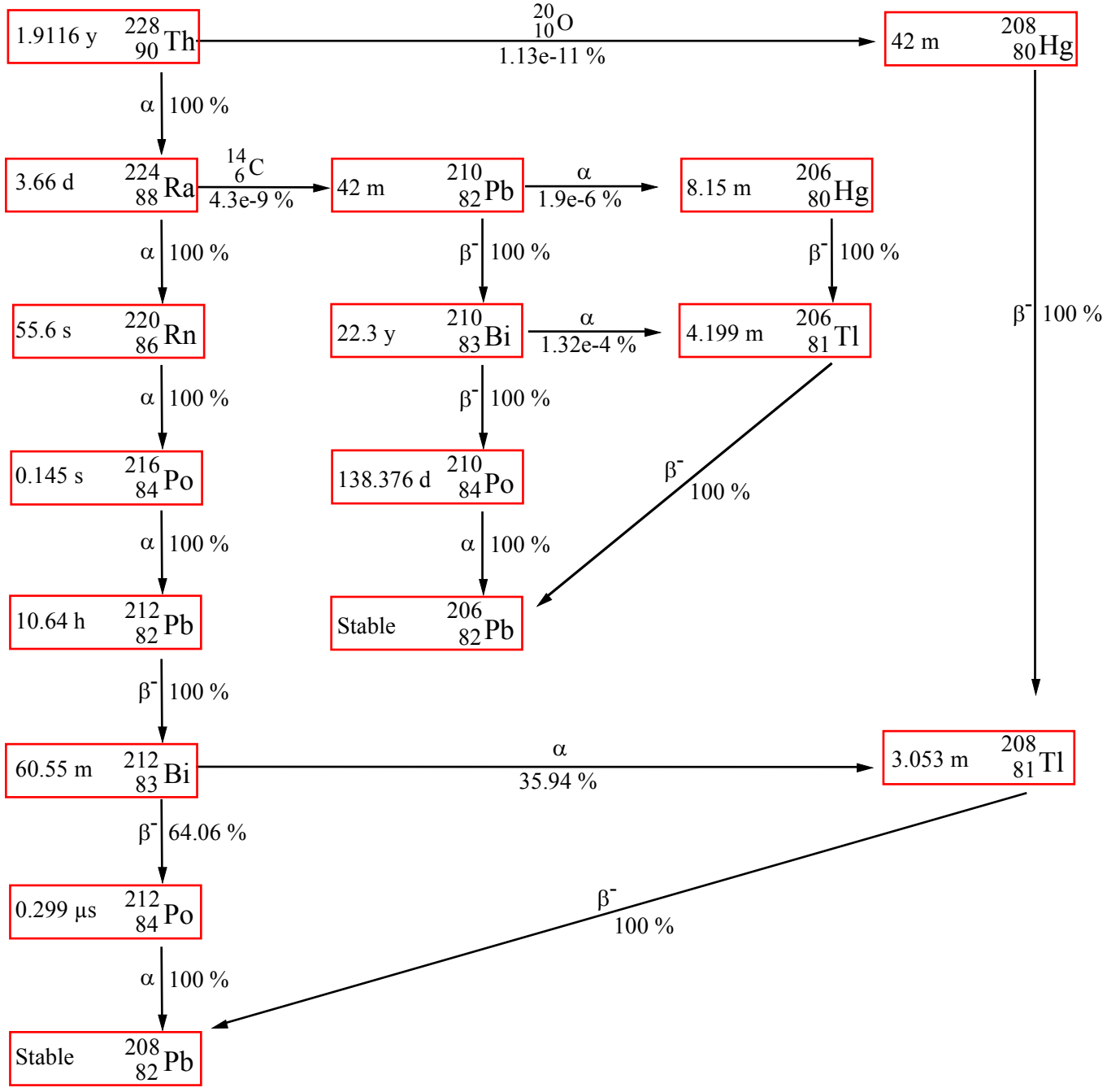

Figure 2-9. Decay chain diagram for ^{228}Th.

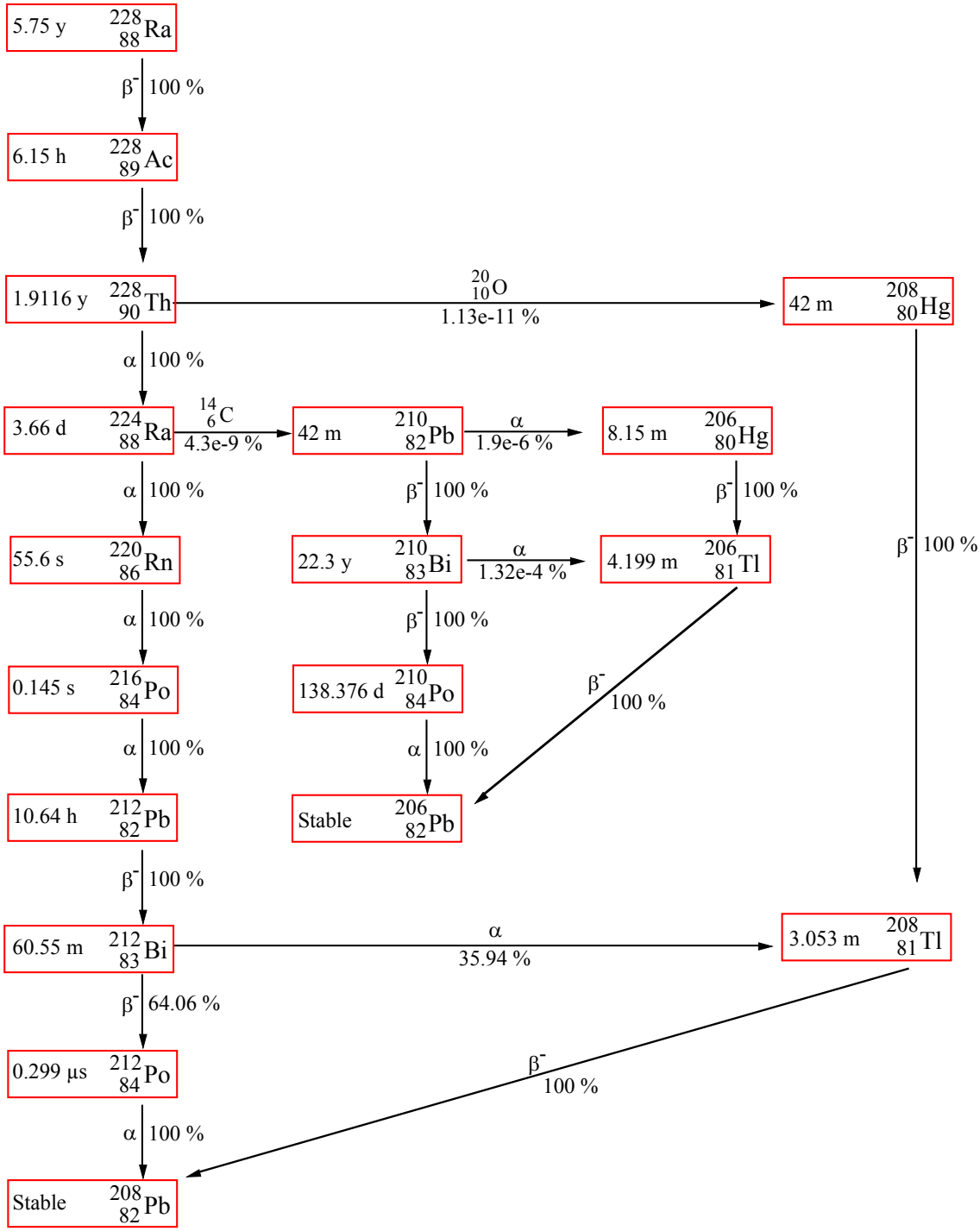

Figure 2-10. Decay chain diagram for ^{228}Ra.

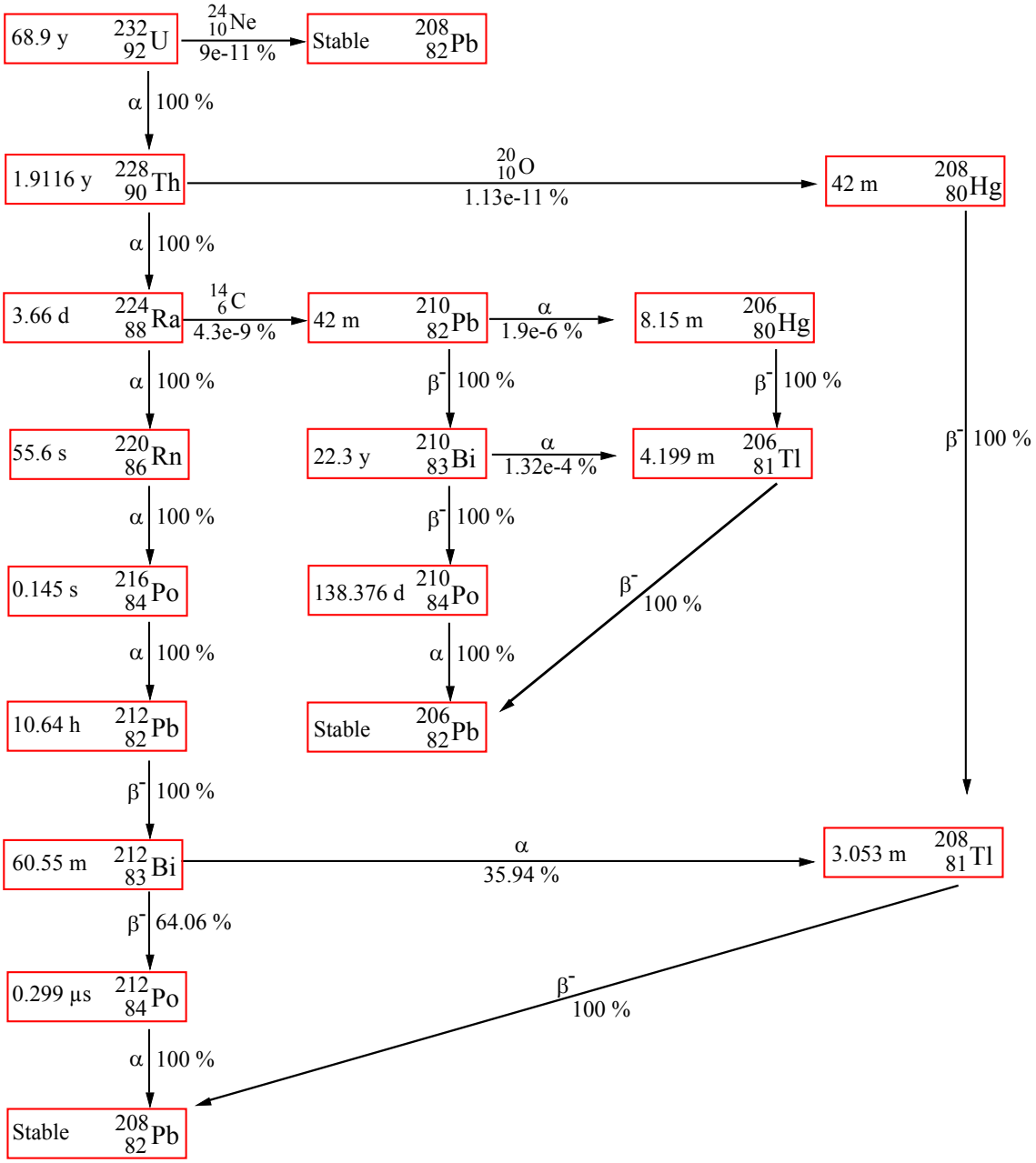

Figure 2-11. Decay chain diagram for ^{232}U.

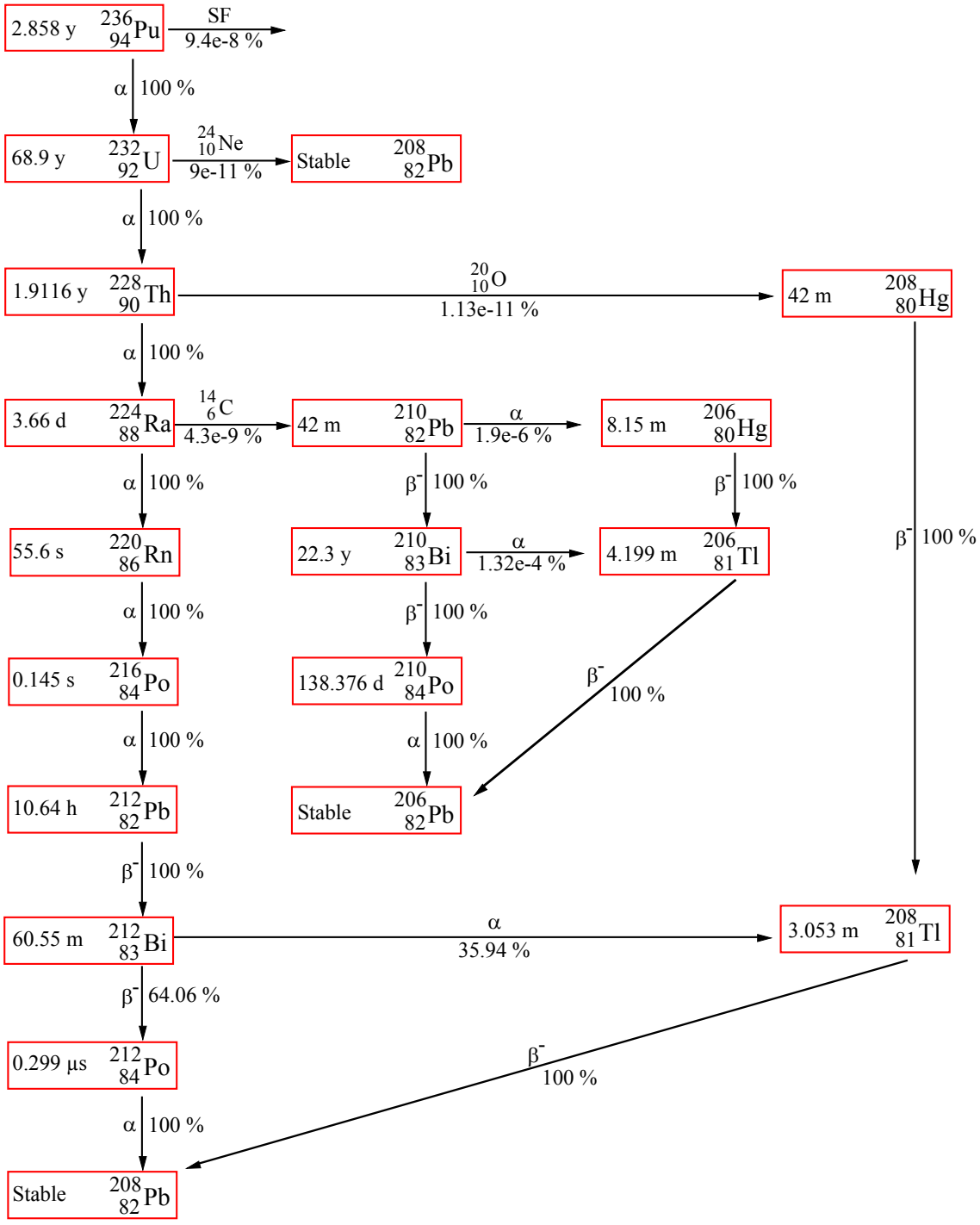

Figure 2-12. Decay chain diagram for ^{236}Pu

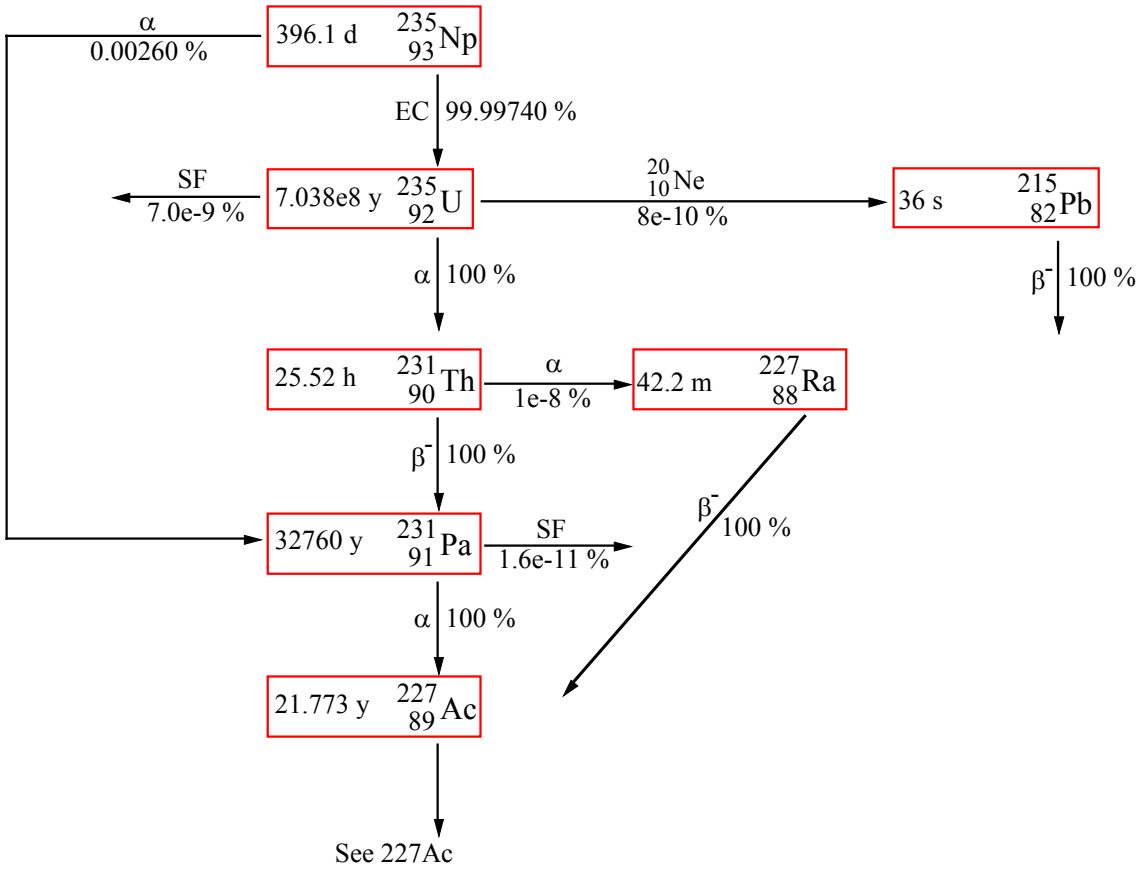

Figure 2-13. Decay chain diagram for ^{235}Np

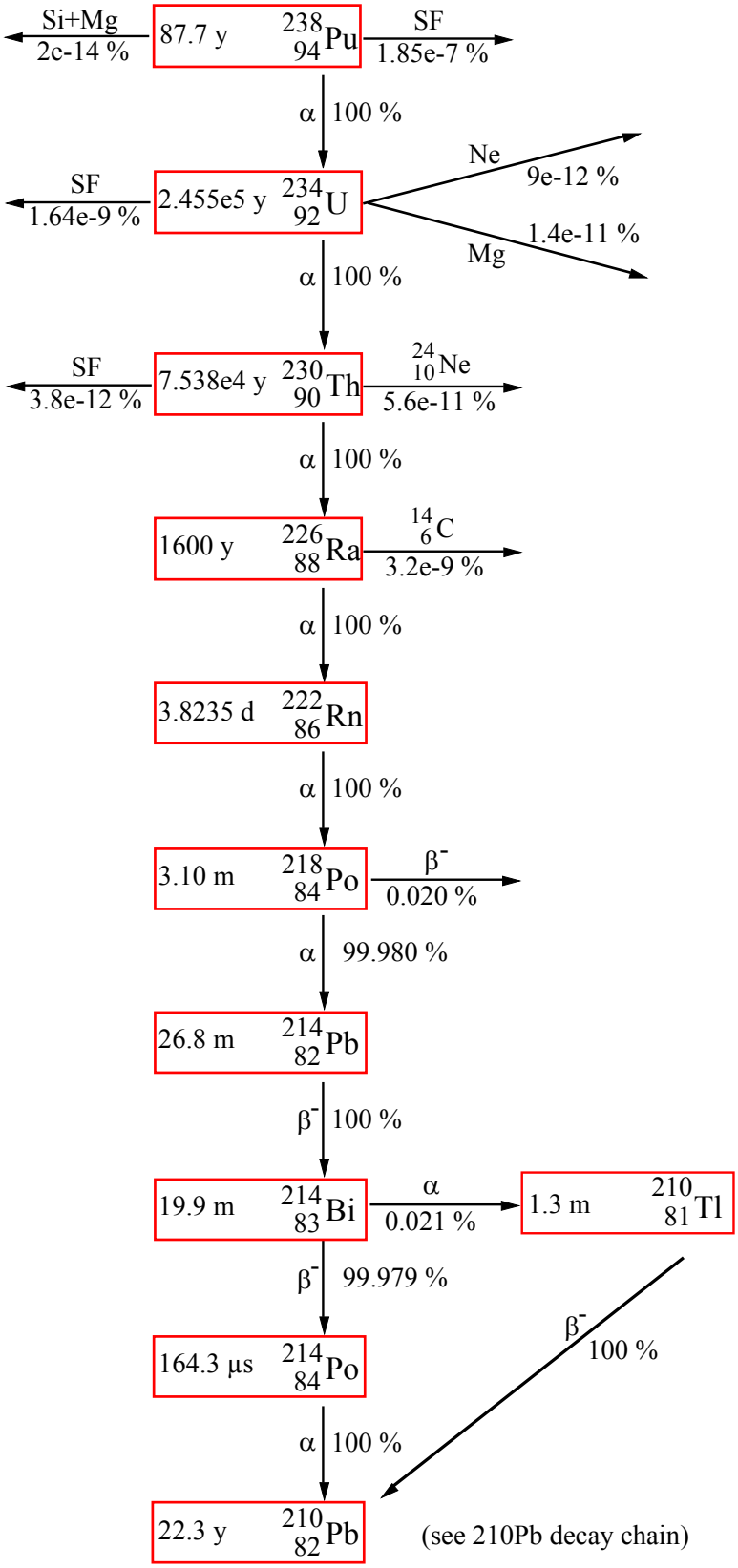

Figure 2-14. Decay chain diagram for ^{238}Pu

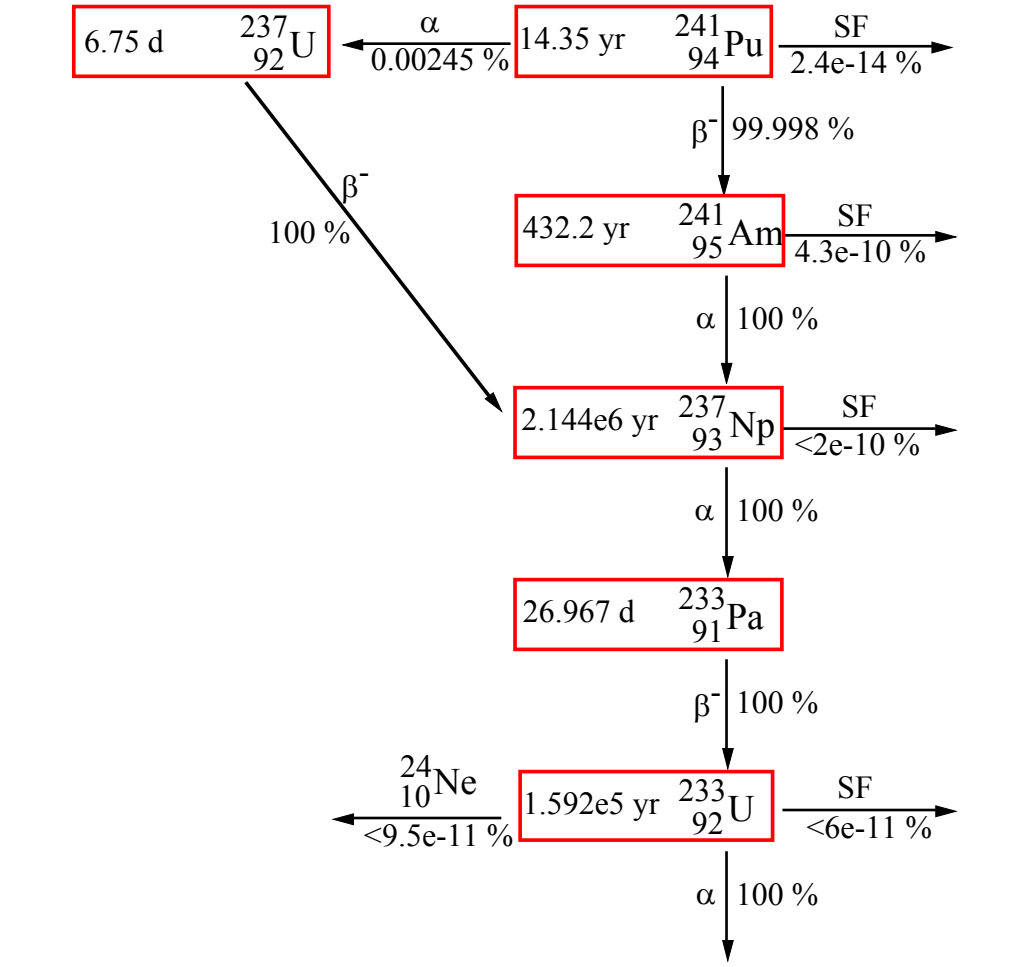

Figure 2-15. Decay chain diagram for ^{241}Pu

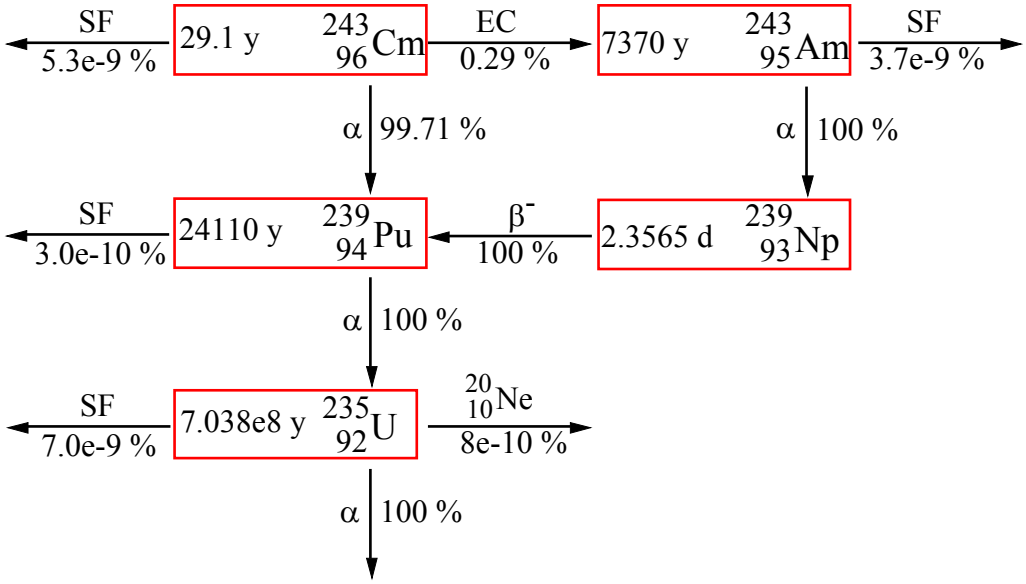

Figure 2-16. Decay chain diagram for ^{243}Cm

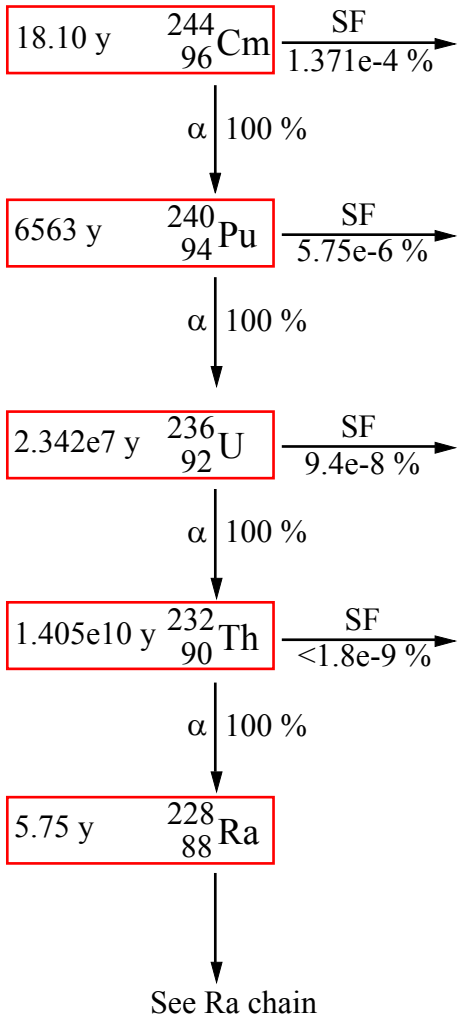

Figure 2-17. Decay chain diagram for ^{244}Cm

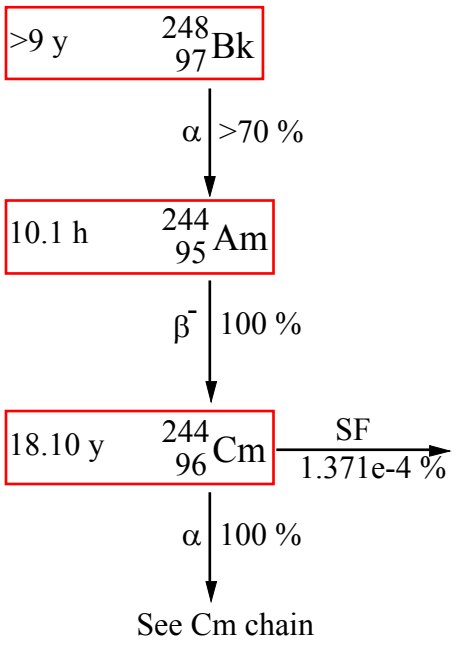

Figure 2-18. Decay chain diagram for ^{248}Bk.

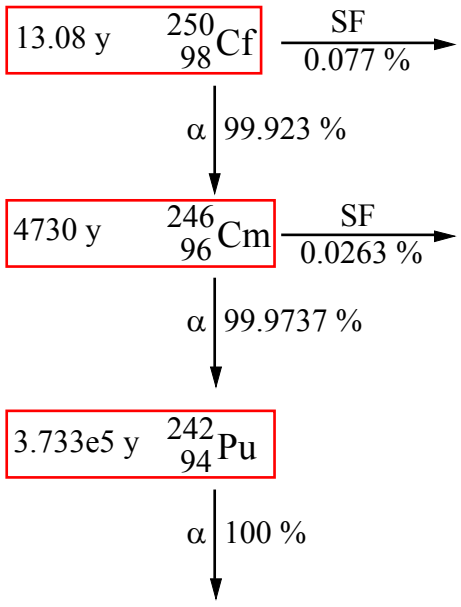

Figure 2-19. Decay chain diagram for ^{250}Cf.

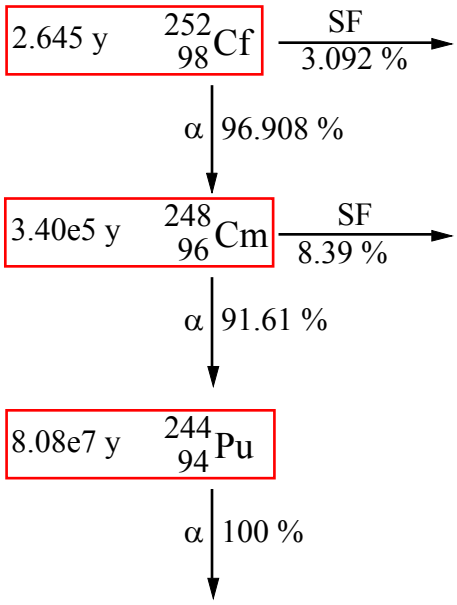

Figure 2-20. Decay chain diagram for ^{252}Cf.

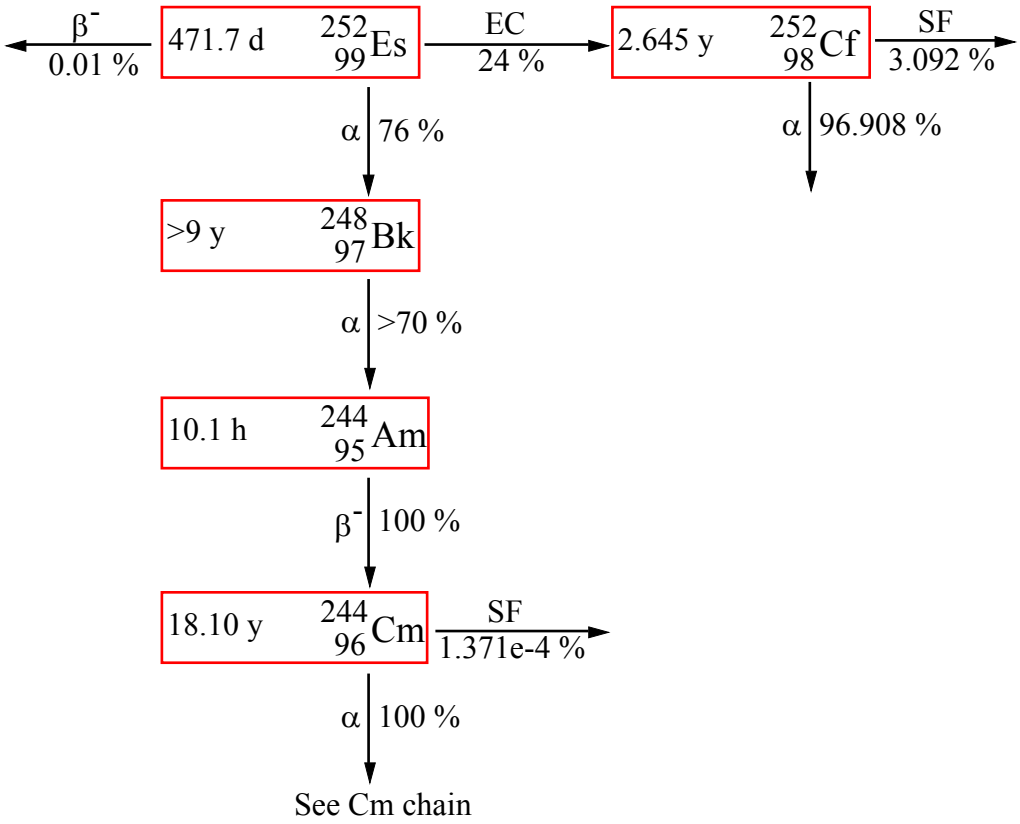

Figure 2-21. Decay chain diagram for ^{252}Es.

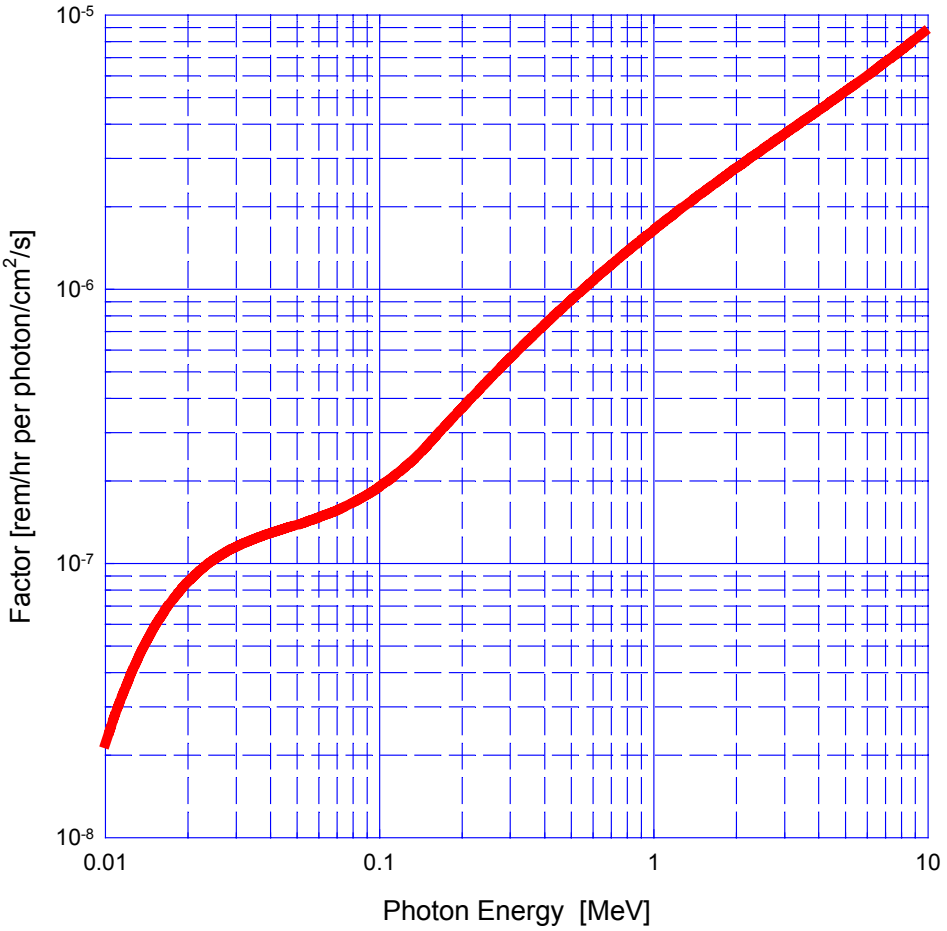

Figure 2-22. Biological dose equivalent of gamma-ray photons as a function of energy. Adapted from values recommended in [ANSI 91]. This chart (or more accurately a vector representing it in computer memory) was used to estimate the biological equivalent dose of various candidate alpha-emitting isotopes due to collateral gamma-ray emission from the decay of daughters to the ground state.

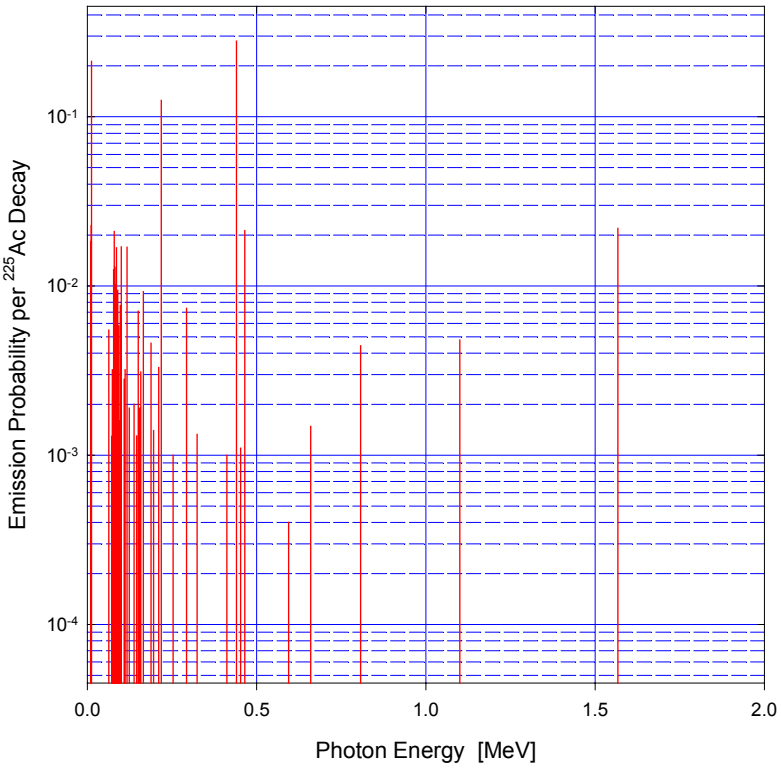

Figure 2-23. Emission probability as a function of energy for gamma-ray photons emitted by ^{225}Ac (a candidate alpha particle emitter for use in a solid state neutron generator) and its daughter isotopes. Compilations of these photon intensity profiles were compiled for all leading candidate alpha-emitting isotopes. Depending on the systematics of the decay of the daughter isotopes, it was sometimes also necessary to compute the emission probabilities at various times from the creation of the pure parent isotope. These probabilities, together with the dose-weighting vector shown in **Figure 2-22** we used to compute the total dose from gamma-rays expected from a candidate alpha emitter.

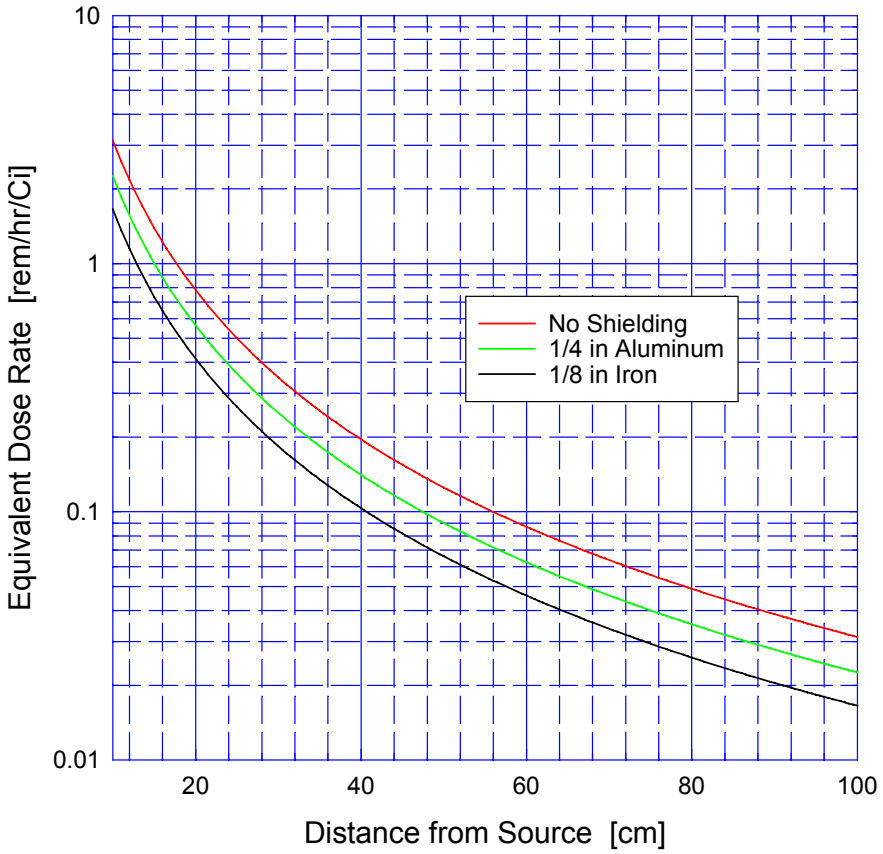

Figure 2-24. Equivalent dose rate for a ^{225}Ac radio-isotopic source as a function of distance from the source. The calculation was also performed with two different shields (iron and aluminum). The computation was performed with shielding material in place because it is unlikely that a neutron generator would ever be deployed in an exposed state. This calculation was normalized to the emission intensity of the source in curies (3.7×10^{10} emissions s^{-1}).

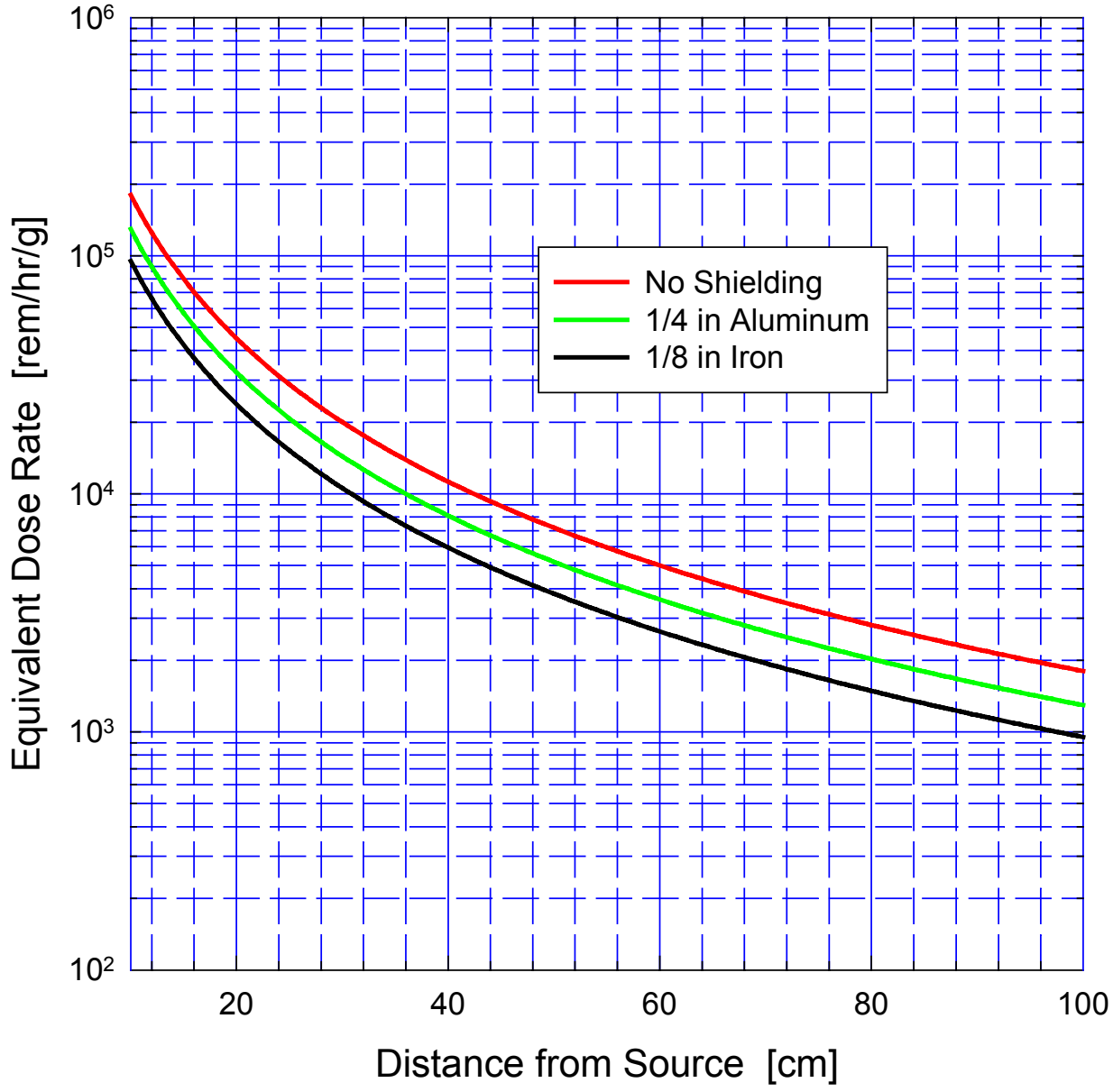

Figure 2-25. Equivalent dose rate for a ^{225}Ac radio-isotopic source as a function of distance from the source. The calculation was also performed with two different shields (iron and aluminum). The computation was performed with shielding material in place because it is unlikely that a neutron generator would ever be deployed in an exposed state. This calculation was normalized to the mass of the source.

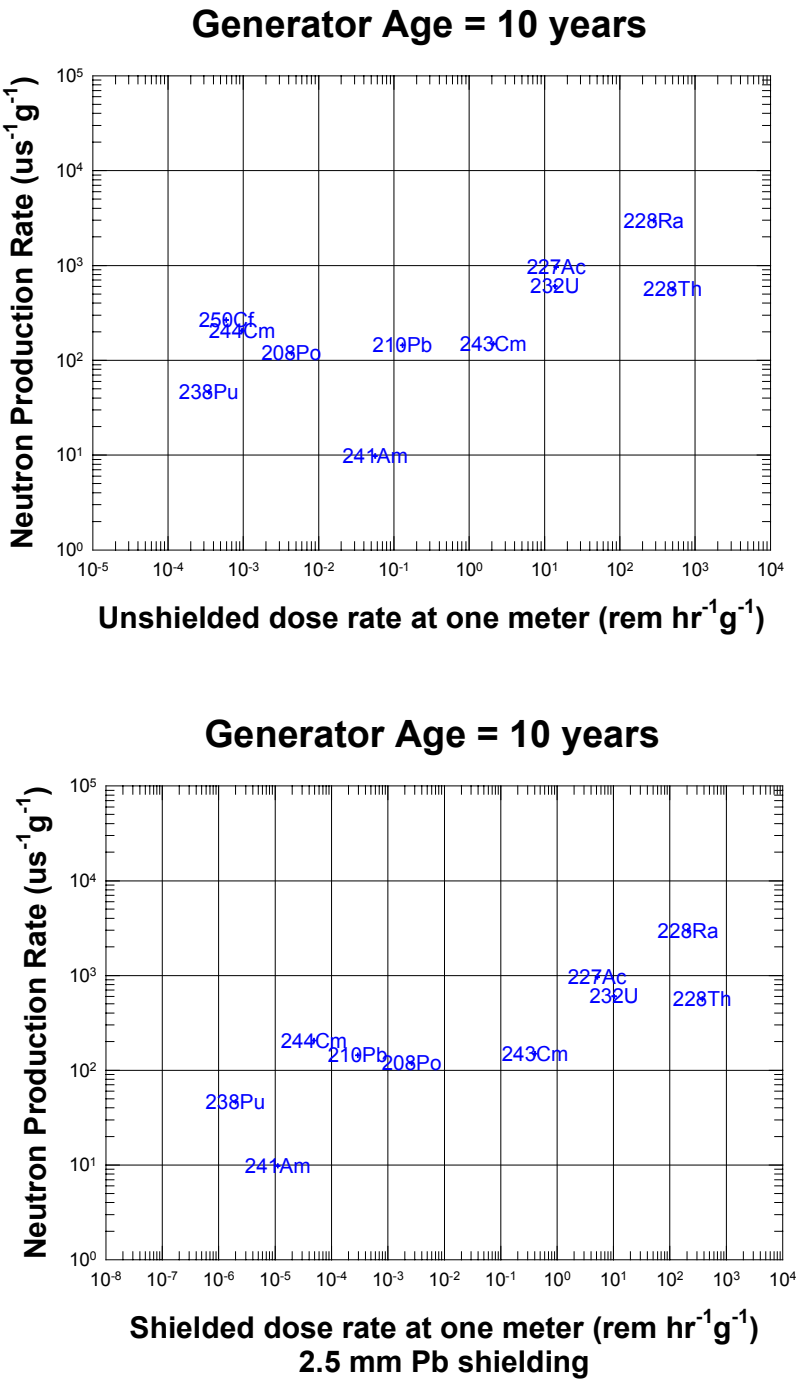

Figure 2-26. Neutron production rate versus gamma-ray dose rate for the leading candidate alpha emitters considered in this study. These calculations were performed at a time of ten years after the creation of the pure parent source. Upper plot is of the bare source configuration, lower graph depicts the situation with a nominal gamma-ray shield in place (2.5 mm of lead).

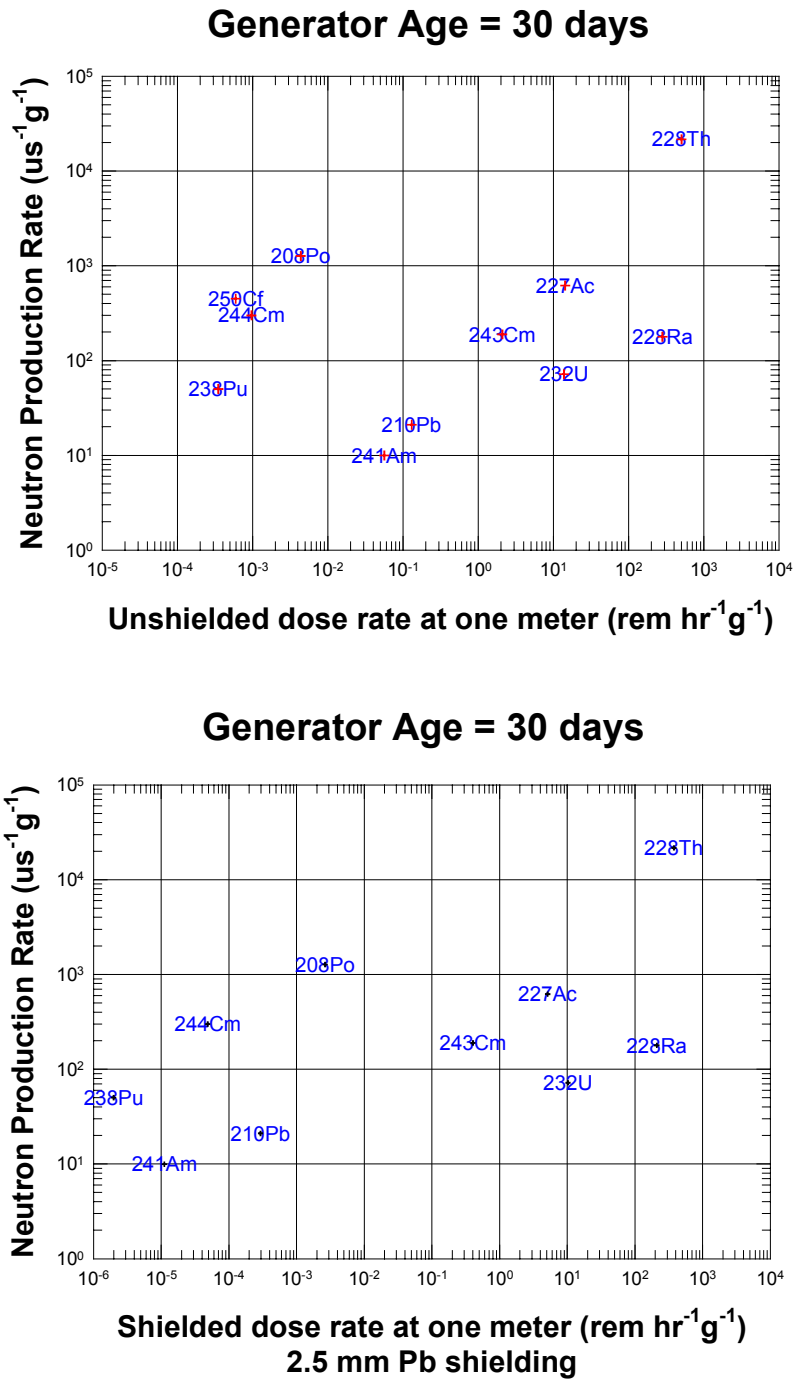

Figure 2-27. Neutron production rate versus gamma-ray dose rate for the leading candidate alpha emitters considered in this study. These calculations were performed at a time of 30 days after the creation of the pure parent source; thus, these calculations represent an estimate of neutron rate versus dose rate for a hypothetical solid state neutron generator at the beginning of its useful life. Upper plot is of the bare source configuration, lower graph depicts the situation with a nominal gamma-ray shield in place (2.5 mm of lead).

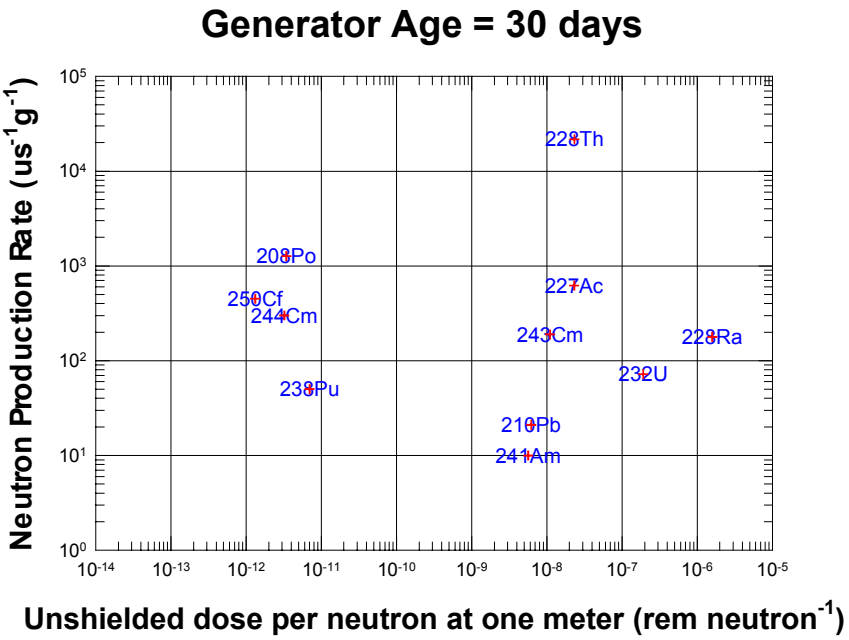

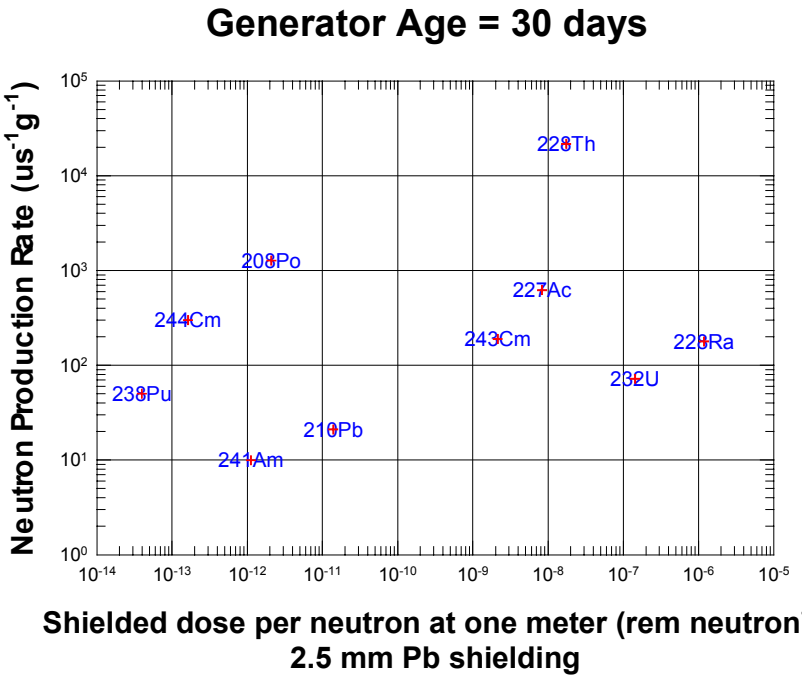

Figure 2-28. Neutron production rate versus gamma-ray dose per neutron for the leading candidate alpha emitters shortly after their production (30 days old) with and without a nominal shield. In this depiction of the tradeoff between neutron production and gamma-ray dose, sources with minimum dose per neutron (left side of graph) are the best. Using this optimization strategy we see that- with moderate shielding- ^{238}Pu is the optimal source for use in an SSNG configuration.

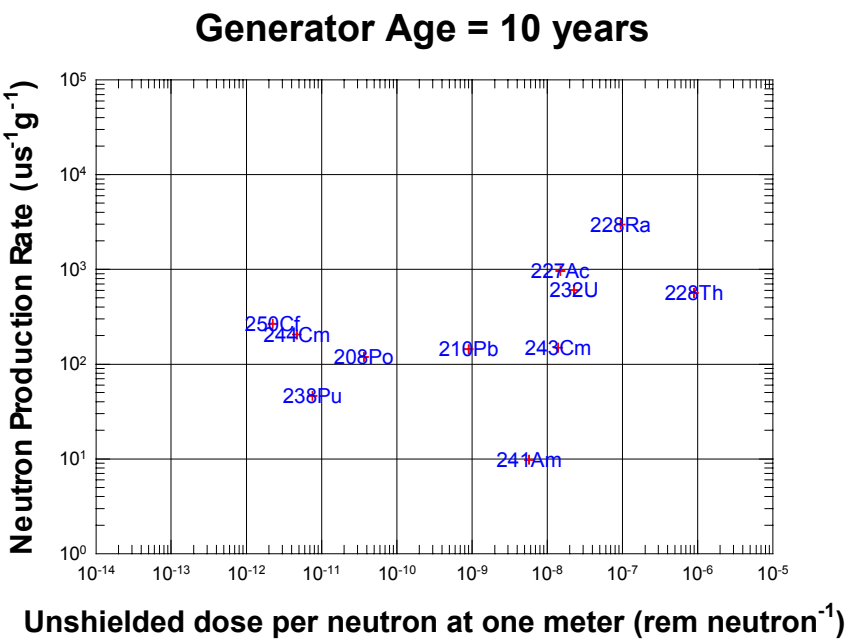

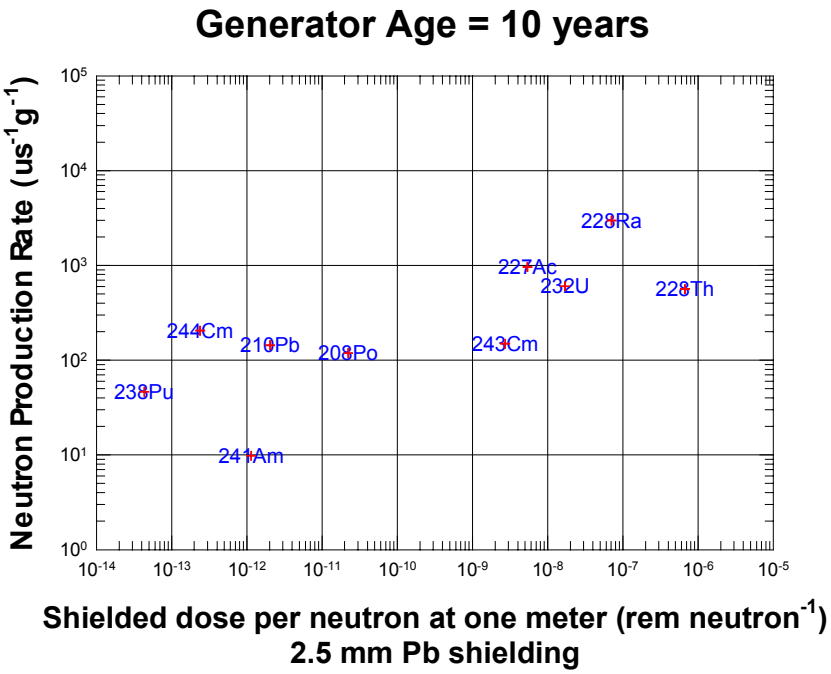

Figure 2-29. Neutron production rate versus gamma-ray dose per neutron for the leading candidate alpha emitters 10 years after their production, with and without a nominal shield. Again we see that- with moderate shielding- ^{238}P is the optimal source for use in an SSNG configuration.

Section 3. Prediction of the Operation of an SSNG

Introduction

A major effort of our research program was the development of a quantitative model to estimate the performance characteristics of a neutron generator before actually building one. After searching unsuccessfully for previously developed computer models of alpha-Be generator performance, we developed our own computation tools for predicting the characteristics of these new devices. Our computation technique involved the creation of a 3-dimensional analog Monte-Carlo computer program to model the transport of alpha particles in the micro-devices. The output of the alpha transport code was then coupled to another computer program, which predicted the distribution of neutrons produced in an energy-angle phase space. Our quantitative methods were later validated by experimental results. In addition to serving the utilitarian role of predicting device performance, the computer codes allowed us to visualize the neutron generation characteristics, and in so doing, create new applications for them.

Before we discuss our detailed simulations, it is worth first reviewing the basics of alpha particle transport and neutron generation in a solid state generator.

Overview of Alpha Particle Transport

Alpha particles are doubly charged helium nuclei. Because they are charged, alpha particles continuously slow down in material media from the moment they are emitted. The rate of energy loss of an alpha particle, $\frac{dE}{dx}$, (often called its "stopping power") may be written as

$$-\frac{dE}{dx} = f(E_\alpha, \rho, Z) \tag{3.1}$$

Where E_α is the energy of the alpha particle, ρ is the density and Z is the atomic number of the material the alpha particle is slowing down in. Various approximate relationships exist for $f(E_\alpha, \rho, Z)$ which are of great historical and theoretical interest (most notably the Bethe Formula) but recently computer codes have evolved which allow us to compute $\frac{dE}{dx}$ with great accuracy for any alpha particle energy and in any material.

Another useful quantity in alpha particle transport theory is the "range" of the alpha particle in a given material. The range may be thought of as the distance required for an alpha particle to lose all of its energy, in other word how far it travels before it stops. Again, computer codes have evolved which predict the range to high precision (by integrating the above stopping power expression). **Figures 3-1** and **3-2** are plots of the range of alpha particles in various materials. Examination of **Figures 3-1** and **3-2** reveals that alpha

particles have a very short range in solid materials; less than 1 mm for any energies we are likely to encounter in this study.

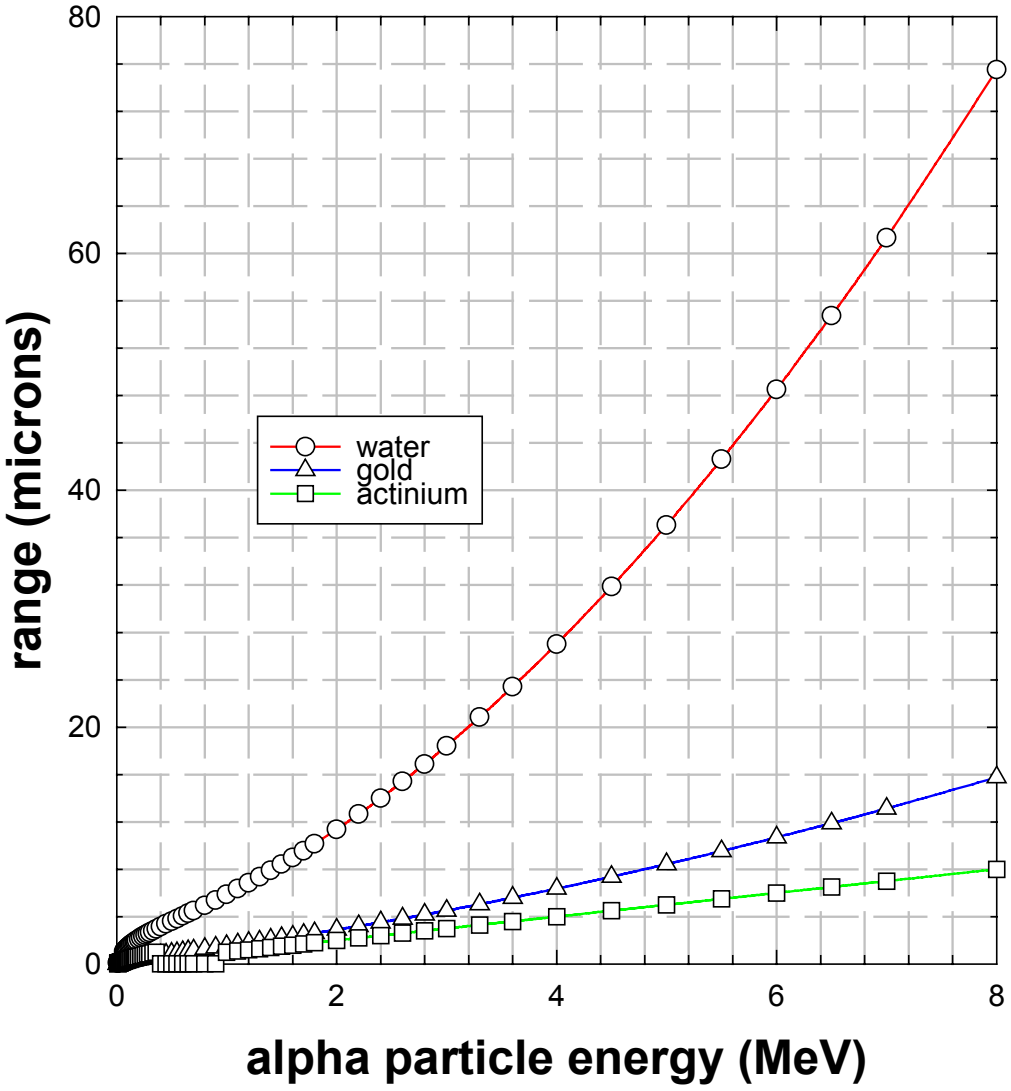

Figure 3-1. Alpha particle range versus energy in three different materials. Actinium was chosen as it is a representative heavy isotope alpha emitter. The range in actinium can be used to estimate the thickness an alpha emitting layer inside a solid state generator can reach before self-attenuation of the alpha particles becomes a problem. The range in gold can be used to estimate the thickness a "stop-plate" must have inside a micro-machined solid state neutron generator. The range of alpha particles in water is shown for comparison purposes.

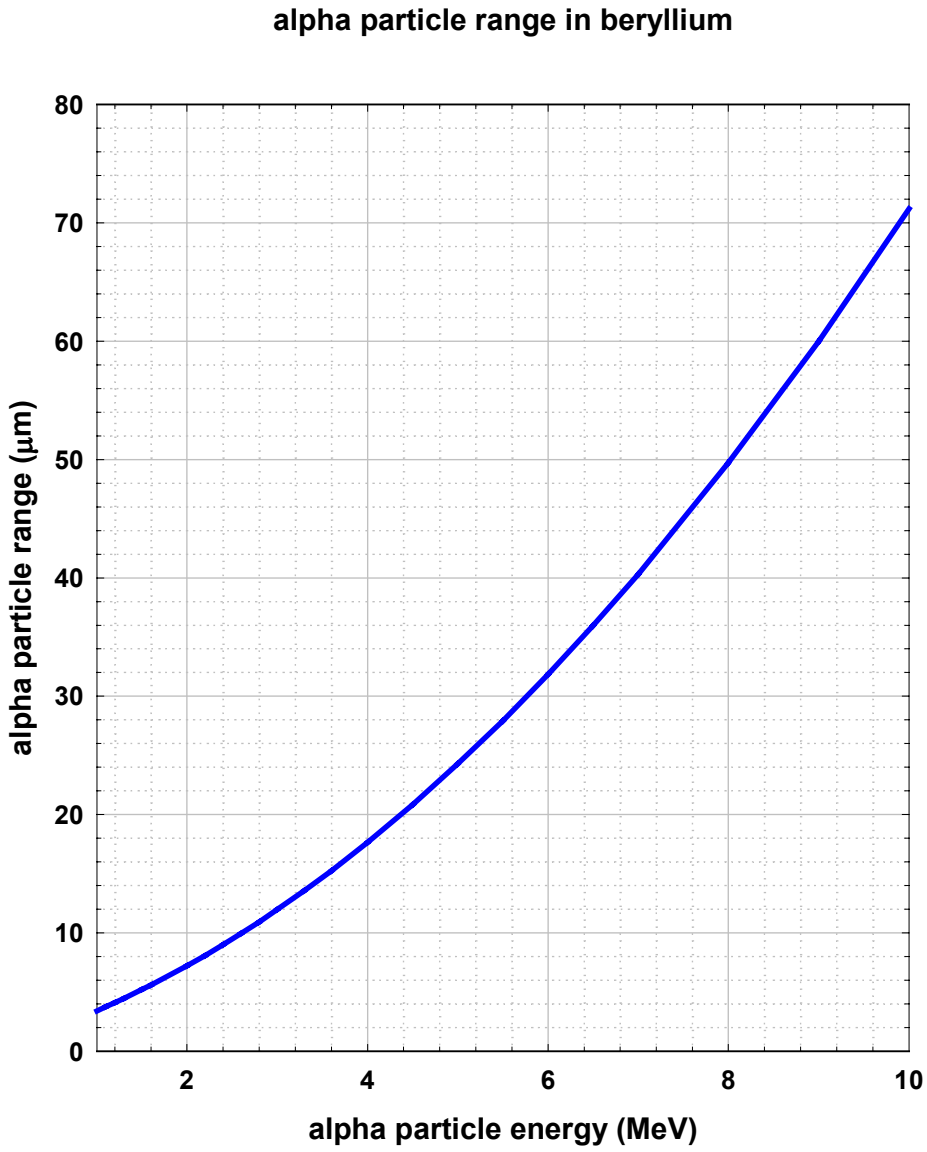

Figure 3-2. Alpha particle range versus energy in beryllium. These data were generated with the code PRAL [Ziegler 85]. The graph can be used to estimate the necessary thickness of a beryllium absorber inside a solid state neutron generator required for efficient neutron generator operation.

Recall that in the solid state neutron generator devices we are designing, alpha particles are produced in a volume of radioactive material and must then travel to a beryllium absorber where they should stop. Furthermore, we want to place a movable barrier between the alpha particle source and the beryllium absorber to switch the neutron generator on and off. Inspection of **Figures 3-1** and **3-2** immediately reveals the approximate dimensions the various components a SSNG must have. We see that the range of 8 MeV alpha particles (the highest energy we are likely to encounter) in actinium is 8 microns. Actinium is very typical of the actinide element alpha emitters examined in this study. Thus we see that our alpha particle sources that we will use in our generators should be thinner than 8 microns. If an alpha particle emitter is thicker than 8 microns none of the alphas generated at a depth of greater than eight microns will ever leave the emitter. Similarly, we see from **Figures 3-1** that the range of 8 MeV alpha particles in gold is 16 microns. Thus we know that if we use a heavy metal shutter in our micro-machined SSNG it need not be any thicker than about 20 microns. Finally, in **Figure 3-2** we see that the range of 8 MeV alpha particles in beryllium metal is 50 microns. Thus, simple range calculations set the approximate dimensions of our SSNG device.

Neutron Generation and Transport

At the length scale of a micro-machined solid state neutron generator, neutron transport is a trivial matter. Basically, the cross-section of energetic neutrons in any material within the generator is so small that, to an excellent approximation, all neutrons created in the generator leave it without interacting at all. However, the mechanics of neutron generation is a much more complicated matter. Unlike the conventional D-T generators which emit neutrons nearly isotropically (the same number in all directions), we found that the neutrons leaving the alpha-Be reaction do so in a very asymmetric manner (with respect to the direction of the incoming alpha particle). The anisotropy of neutron emission was never examined in conventional alpha-Be generators because, in these devices, the alpha particles are likely to strike the Be nuclei at any angle, thus the macroscopic generator is isotropic even when the individual alpha-Be reactions are not. However, in a micro-fabricated generator, the range of angles at which the alpha particles strike the beryllium target is likely to be constrained; thus we expect the angular distribution of neutrons from the generator to be anisotropic. Although the anisotropy of neutron emission tremendously complicates the calculation of SSNG response, it also offers unique opportunities for new applications.

Steps in the Prediction of SSNG Behavior

Our prediction of the behavior of a neutron generator involves three steps. Computation of the transport of alpha particles out of the emitting isotope layer and through the generator parts. Computation of the angular distribution of neutrons in the Be layer. And, finally, the folding of the alpha transport with the neutron distribution results to predict the actual energy and angle distribution of neutrons leaving the generator. In addition to these three steps, additional computation is required to compare the results of the prediction with experimental results (due to the imperfect nature of the neutron detector used in the experiments).

Alpha Particle Transport in an SSNG

We chose a straightforward analog Monte Carlo method to model the behavior of alpha particles in a hypothetical solid state neutron generator. The first step in the simulation was to model the emission of the alpha particle from an isotope in the emitting layer. This modeling was performed by stochastically sampling the various emission energies of the alpha emitter (with the correct probability distribution to mimic the average isotopic emission intensities). Once an emission energy was chosen, a random direction was chosen for alpha particle emission. Spherical coordinates were used in the emission process analog with one angle sampled uniformly (by a random number generator) and the other sampled with an inverse cosine generator to produce isotopic emission. Once the emission angles were chosen, the intersections of the alpha track with the surface of the emitter and with the beryllium absorber were calculated. If it was found that the alpha particle was not going to hit the beryllium absorber, no further computation was performed (but a tally was kept of the emission) and a new "particle history" was begun. If it was found that the alpha particle might hit the beryllium, its energy loss traveling to the surface of the emitter was computed. Of course if the alpha particle lost all of its energy on the way to the surface, the history was terminated and the no-hit tally was incremented. Finally, if the alpha made it to the beryllium surface with non-zero energy, an array tally was kept of the energy distribution and angular distribution that the particle made with the surface. Visualizations and plots of some of the tallies produced with the alpha particle transport simulation program are shown in **Figures 3-3** to **3-8**.

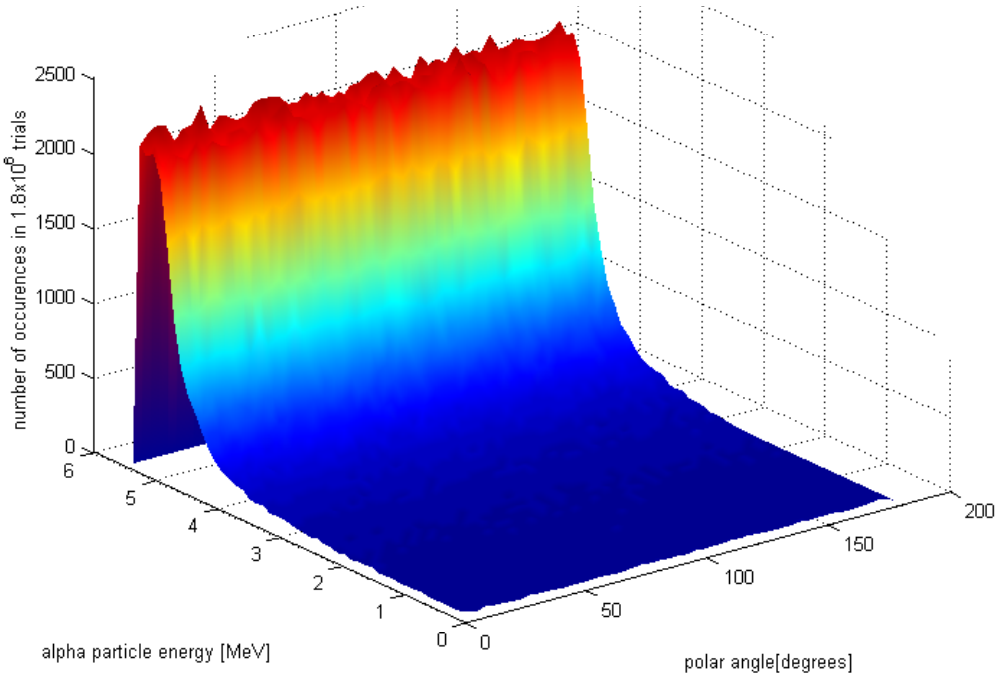

Figure 3-3. Two-dimensional histogram of the event frequency of alpha particle emission versus energy and emission angle for a 2 micron thick ^{241}Am source (approximately mono-energetic alpha emitter at 5.5 MeV). This simulation comprised 1 million iterations of the Monte Carlo transport code and assumed essentially infinite sheets of alpha emitter and beryllium separated by a vacuum.

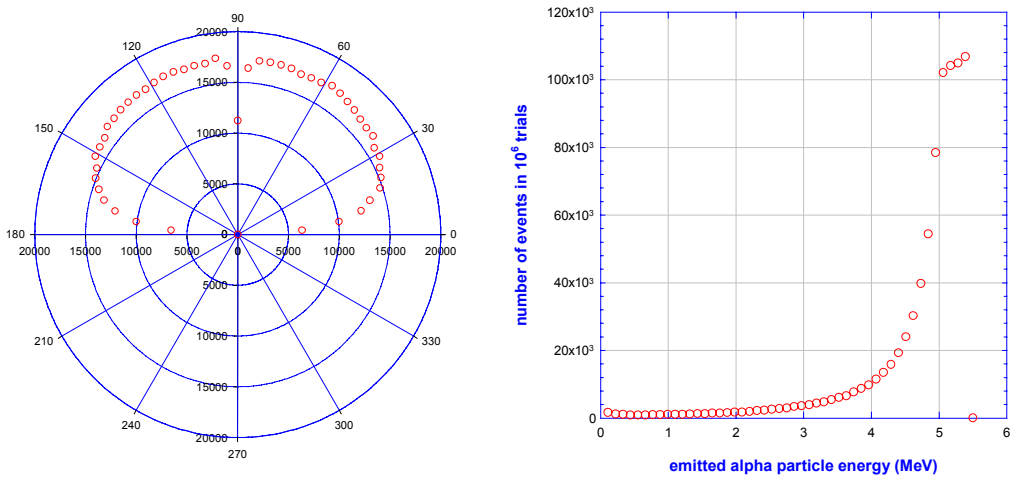

Figure 3-4. **A**. Computed angular distribution of alpha particles for the infinite 2 micron ^{241}Am source. **B**. Computed energy distribution of alpha particles emerging from the infinite 2 micron thick ^{241}Am emitter. Note that for an infinitesimally thin ^{241}Am layer we would expect the energy distribution to be a delta function at 5.5 MeV.

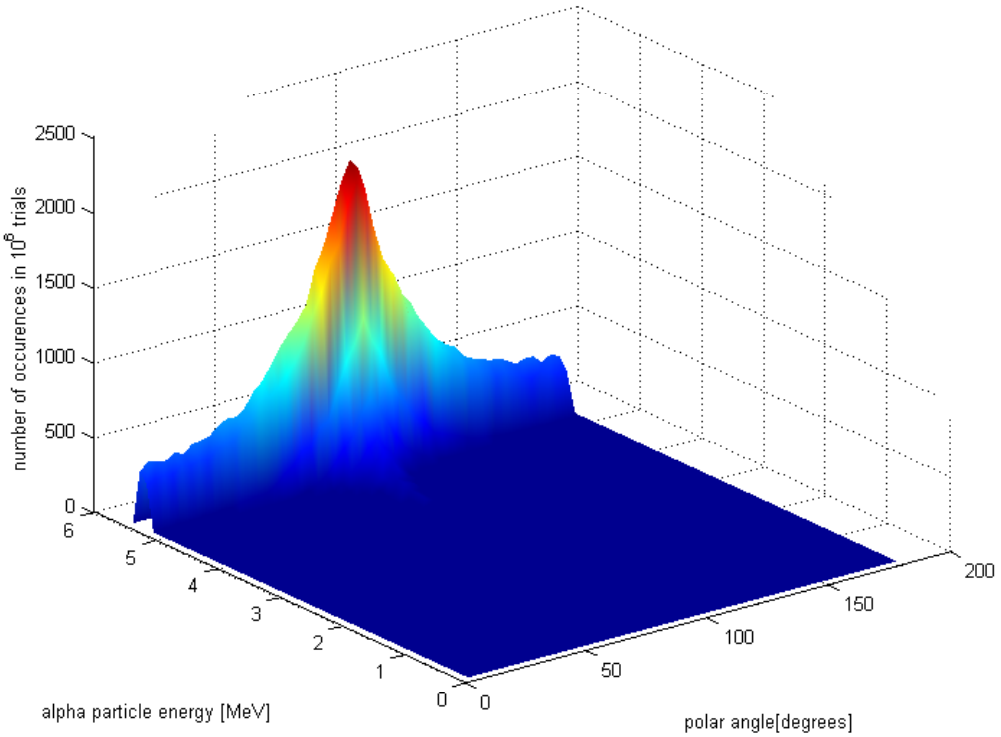

Figure 3-5. Two-dimensional histogram of the event frequency of alpha particle emission versus energy and emission angle for a one micron thick ^{241}Am source. The source was inside a hypothetical micro-fabricated gold well of the same dimensions as one fabricated later in the project (see **Figures 4-15** and **4-16).**

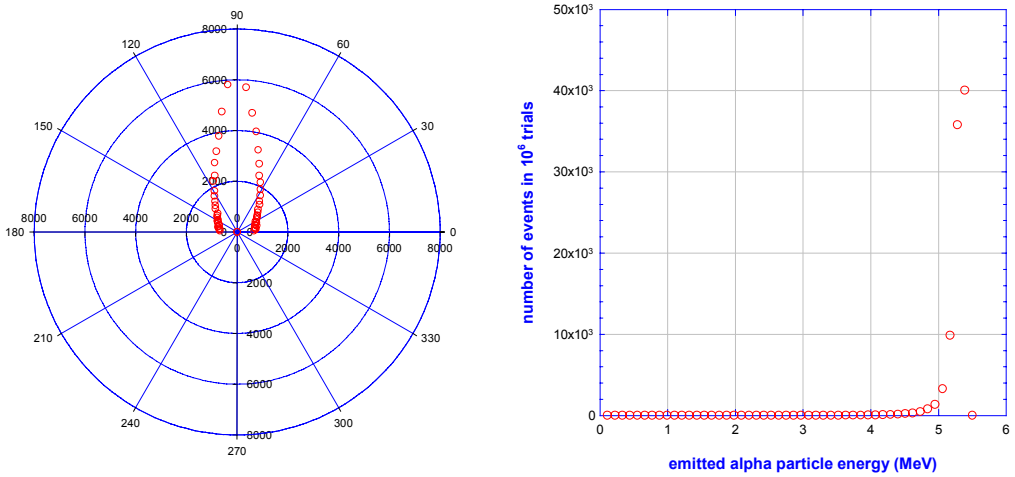

Figure 3-6. **A**. Computed angular distribution of alpha particles for the 1 micron ^{241}Am well source. **B**. Computed energy distribution of alpha particles emerging from the 1 micron ^{241}Am well source. Note that for an infinitesimally thin ^{241}Am layer we would expect the energy distribution to be a delta function at 5.5 MeV

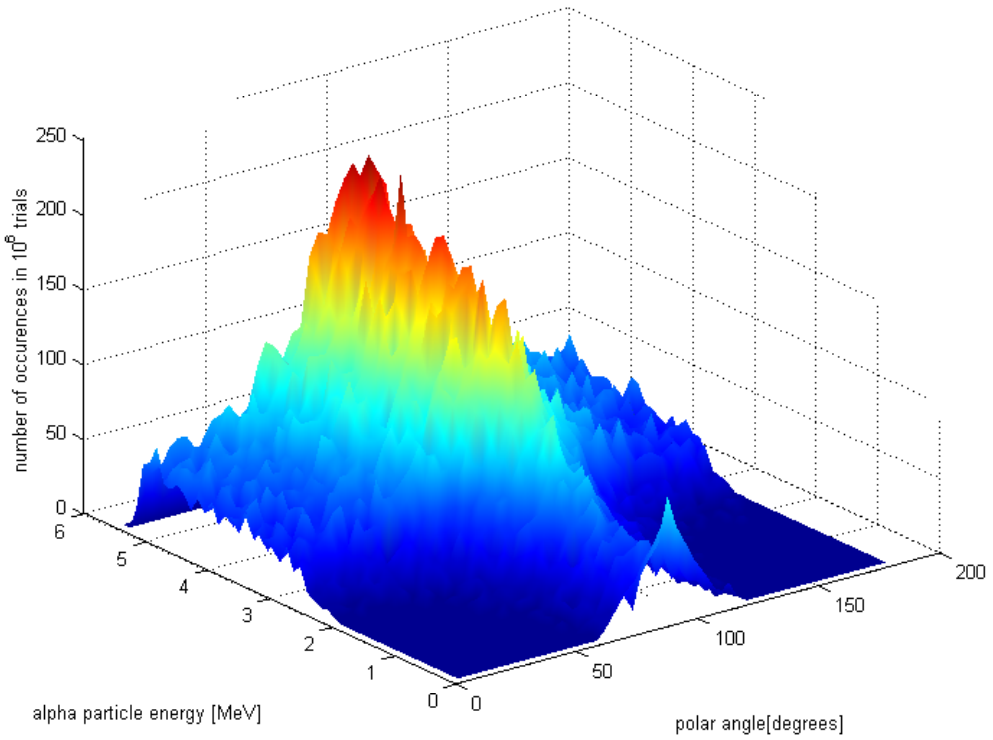

Figure 3-7. Two-dimensional histogram of the event frequency of alpha particle emission versus energy and emission angle for a ten micron thick ^{241}Am source. The source was inside a hypothetical micro-fabricated gold well of a beryllium absorber inside a solid state neutron generator required for efficient neutron generator operation.

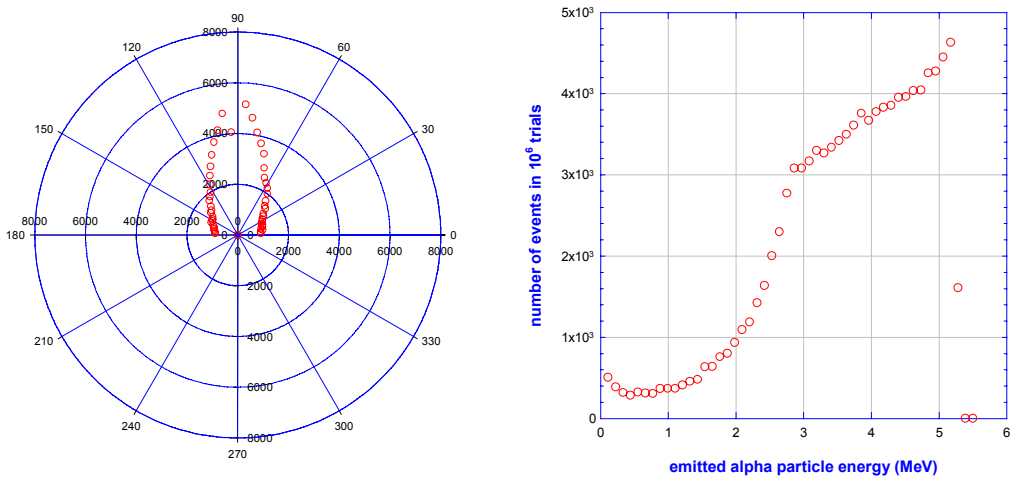

Figure 3-8. **A**. Computed angular distribution of alpha particles for a 10 micron ^{241}Am source inside a gold well. **B**. Computed energy distribution of alpha particles emerging from a 10 micron ^{241}Am source inside a gold well. Note that for an infinitesimally thin ^{241}Am layer we would expect the energy distribution to be a delta function at 5.5 MeV

Neutron Emission Distribution

The next step in the SSNG simulation process was to estimate the angular distribution of neutrons created in the beryllium layer. We modeled the angular distribution by downloading experimentally determined angular distributions and then interpolating between the distributions with Legendre polynomials. Some snapshots of these calculations taken over the range of energies of the possible alpha emitting isotopes are shown in **Figures 3-9** to **3-12**. Examination of these figures reveals the rise in complexity of the neutron energy-angle pattern as the incident alpha particle energy increases. This increase in complexity is due to the excitation of energetic levels in the target ^{7}Be target nucleus and, in some instances, reactions that leave the product nucleus (^{12}C) in an excited state.

It is worth emphasizing that the neutron emission distributions computed here are highly idealized. They represent the neutron emission distribution obtained when mono-energetic alpha particles are normally incident on a very thin foil of beryllium. In the next section of this report (when we analyze the experimental data), we will have to modify the form of the neutron emission distributions to account for the slowing of the alpha particles in thick targets of beryllium. For clarity, and continuity of notation, we point out that the emission distributions shown in **Figures 3-9** to **3-12** are represented in the next section of this report by the form:

$$\Phi^{n}_{thin}(\phi_{\alpha} = 0^{o}, E^{0}_{\alpha}, \phi_{n}, E_{n}) \qquad (3.2)$$

where ϕ_{α} is the angle of incidence of the alpha particle on the beryllium target, E^{0}_{α} is the specific energy of the alpha particle impinging on the target (constant in this case), and ϕ_{n} and E_{n} are the emission angle and energy of the emitted neutron. In the next section of this report we will modify these distributions to account for the more complicated situation encountered in the laboratory.

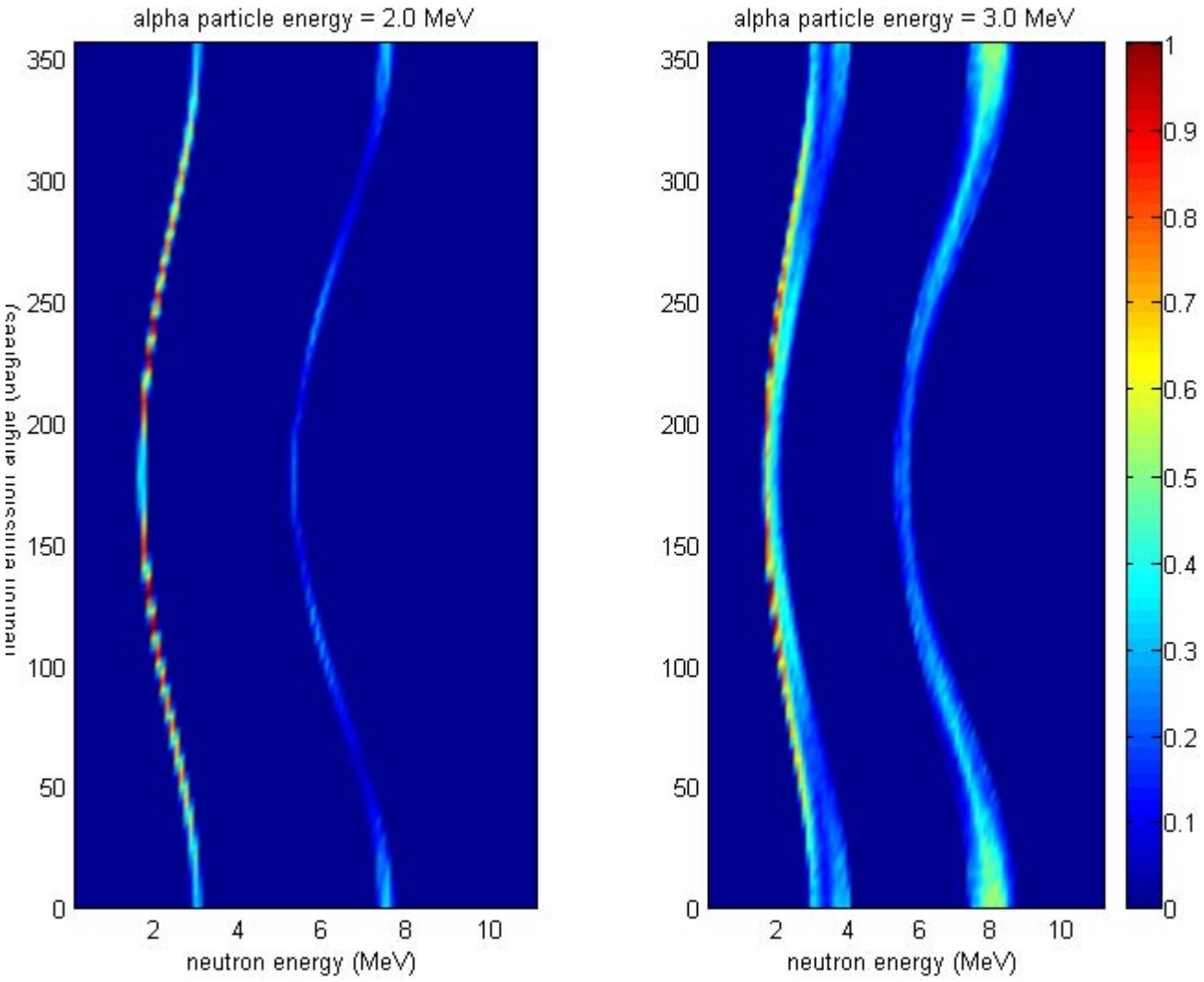

Figure 3-9. Distribution of neutrons as a function of neutron energy and neutron emission angle from the alpha-Be reaction. The plot on the left is for a 2.0 MeV incident alpha particle energy, $\Phi^{n}_{thin}(\phi_{\alpha}=0^{o}, E_{\alpha}=2MeV, \phi_{n}, E_{n})$, and the plot on the right is for a 3.0 MeV alpha particle energy, $\Phi^{n}_{thin}(\phi_{\alpha}=0^{o}, E_{\alpha}=3MeV, \phi_{n}, E_{n})$

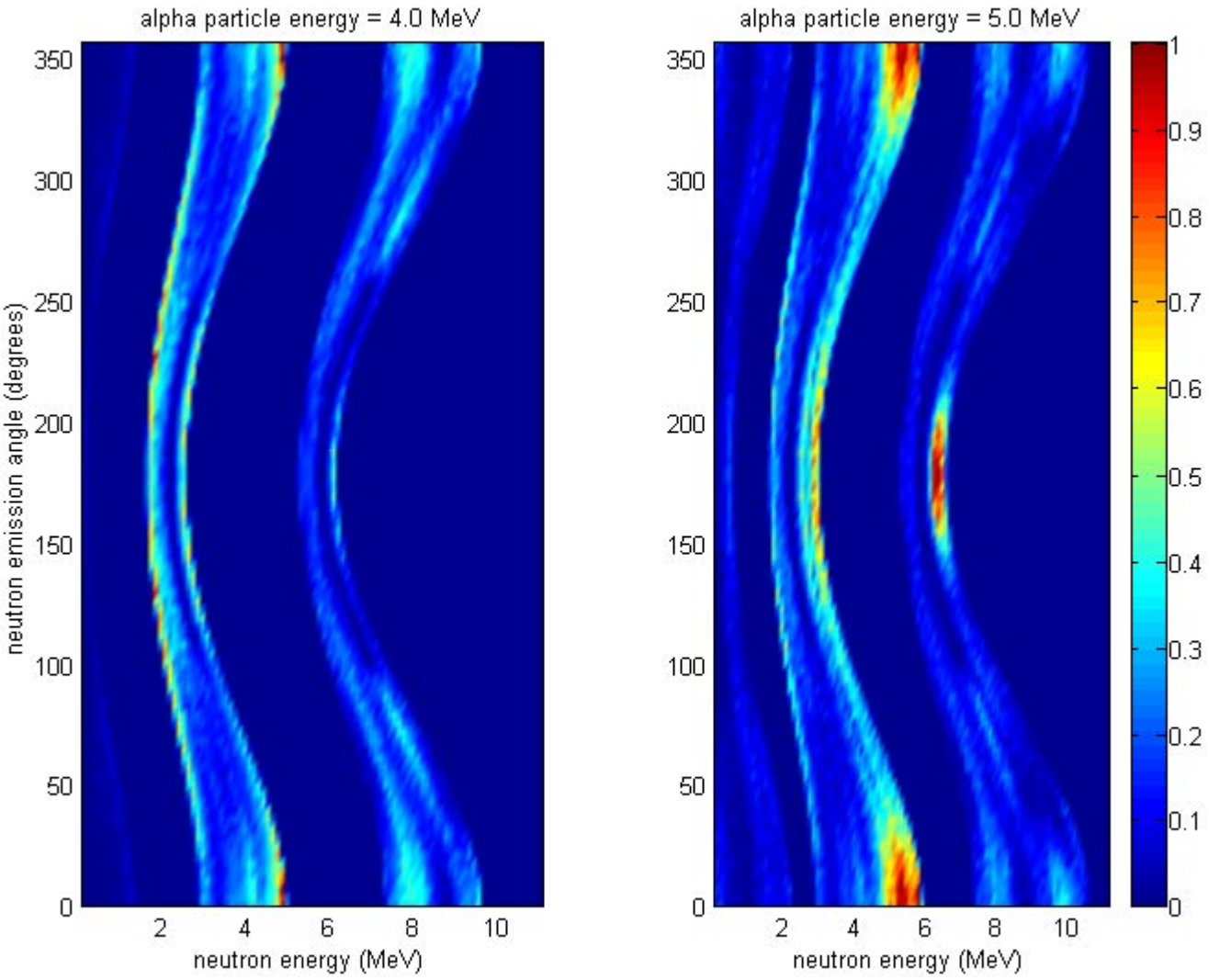

Figure 3-10. Distribution of neutrons as a function of neutron energy and neutron emission angle from the alpha-Be reaction. The plot on the left is for a 4.0 MeV incident alpha particle energy and represents the function $\Phi^{n}_{thin}(\phi_{\alpha}=0^{o}, E_{\alpha}=4MeV, \phi_{n}, E_{n})$, and the plot on the right is for a 5.0 MeV alpha particle energy, $\Phi^{n}_{thin}(\phi_{\alpha}=0^{o}, E_{\alpha}=5MeV, \phi_{n}, E_{n})$

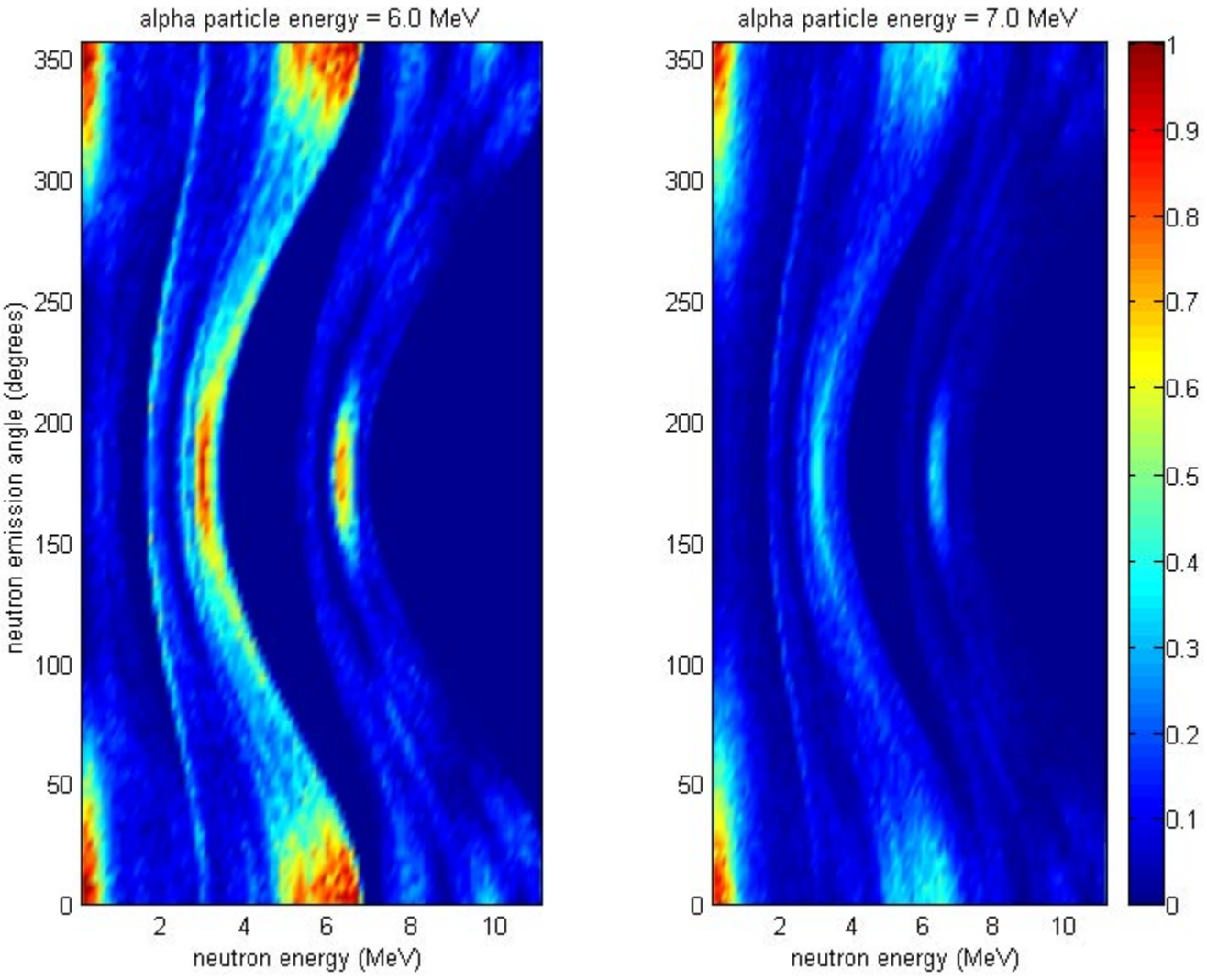

Figure 3-11. Distribution of neutrons as a function of neutron energy and neutron emission angle from the alpha-Be reaction. The plot on the left is for a 6.0 MeV incident alpha particle energy and represents the function $\Phi^{n}_{thin}(\phi_\alpha = 0^o, E_\alpha = 6MeV, \phi_n, E_n)$, and the plot on the right is for a 7.0 MeV alpha particle energy, $\Phi^{n}_{thin}(\phi_\alpha = 0^o, E_\alpha = 7MeV, \phi_n, E_n)$. The 6 MeV distribution resembles one of the experimental situations encountered (5.5 MeV alphas from ^{241}Am) and discussed in the next section of this report.

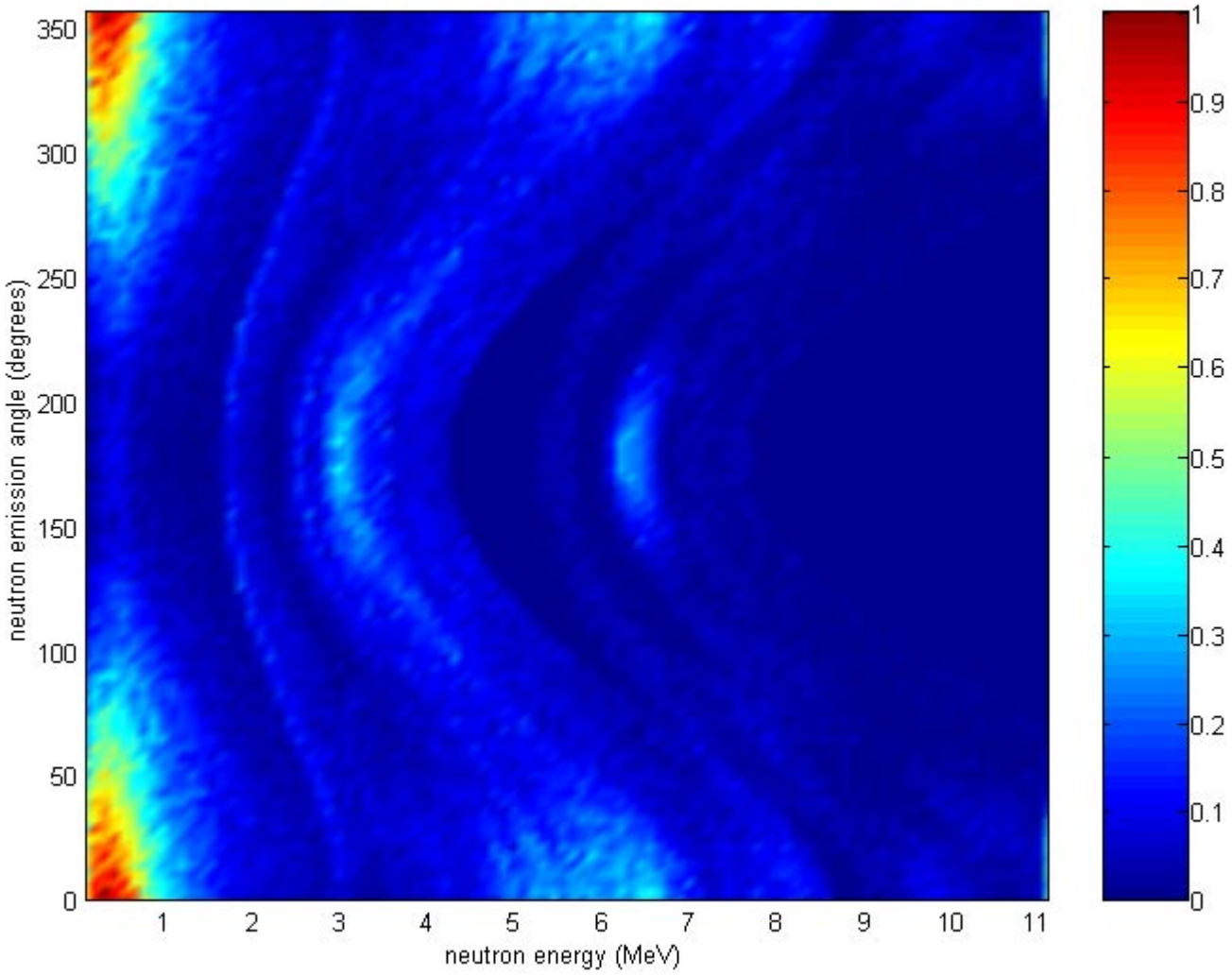

Figure 3-12. Distribution of neutrons as a function of neutron energy and neutron emission angle from the alpha-Be reaction. This plot of neutron emission intensity as a function of neutron emission angle and emitted neutron energy is for a 8.0 MeV incident alpha particle energy and represents the function $\Phi^{n}_{thin}(\phi_{\alpha}=0^{o}, E_{\alpha}=8MeV, \phi_{n}, E_{n})$. 8.0 MeV was the highest alpha particle energy considered in this study, as it is about the highest energy encountered for a long-lived (greater than one day) alpha-emitting radioisotope. Note the complexity of the emission distribution; especially compared to the low energy distributions illustrated in **Figure 3-9**.

Section 4. Experimental Results

Introduction

In this chapter we describe the culmination of our research into switchable, micro-machined SSNGs with a description of the experimental results. These results are divided into two general areas. The first area is the experiments that were performed to validate the theory described in the last section of this report (Section 3.). The second area of research described in this section is the fabrication of micro-machined parts.

Demonstration Experiments

Two major experiments were performed to test the validity of our theories of solid state neutron generator operation. The first experiment entailed the use of a relatively simple alpha-particle emitter (^{241}Am) irradiating a disc of beryllium. This first experiment was important because it was much easier to validate theoretically than the subsequent experiment. To first order, ^{241}Am may be considered a mono-energetic alpha particle emitter (5.5 MeV), and this quality made the neutron transport calculations much simpler and less prone to error.

The second experiment involved the use of ^{225}Ac, a short-lived alpha emitter ($t_{1/2}$ = 10 days). The ^{225}Ac experiment was far more complex to execute, and far more difficult to analyze, as well. ^{225}Ac and its daughters emit a very complex distribution of alpha particles and the transport calculations were necessarily more complicated than for ^{241}Am. However, the total neutron output from the ^{225}Ac was expected to be much higher than with ^{241}Am, and thus we expected much better statistics with which to interpret the more complex results.

Americium-241 - Beryllium

A diagram of the ^{241}Am -beryllium experiment is shown in **Figure 4-1**, and a photograph of some of the apparatus used to perform the experiment is shown in **Figure 4-2**. As **Figure 4-1** illustrates, the "Am-Be" experiment consisted of placing a ^{241}Am source in close proximity to a Be foil, and monitoring the resulting neutron emission with a detector moving in a circular arc.

The ^{241}Am source was mounted 6 mm away from a 2.5 cm x 2.5 cm x 3 mm thick piece of beryllium, and the source/target assembly was mounted in a vacuum chamber to minimize energy loss of the alpha particles as they traveled to the beryllium. Three detectors were mounted on a computer controlled 7 in. (17.8 cm) long pivot arm. The axis of the pivot was located on the Be target.

The primary detector used in the Am-Be experiment was a 2 in. diameter by 2 in. thick cylindrical liquid scintillator (Bicron BC-501A) mounted to a fast 2 in. photo-multiplier tube; this detector assembly was fabricated and tested at SNL/CA. The detector was run in a pulse shape discrimination mode, which allowed it to discriminate neutron counts from gamma-ray background very effectively.

Two other commercial gas filled neutron detectors were used in the Am-Be experiment but neither of these detectors were functional at the time of the Am-Be experiment. Later, we were able to correctly configure these two detectors and they are described later in this report in the description of the ^{225}Ac experiment.

The Am-Be experiment was run, under computer control, for 63 hours. The software that ran the experiment moved the pivot arm through an arc of 200 degrees in 21 positions spaced 10 degrees apart. Data were acquired for 3 hours at each position. An analysis of these data, and comparison with experiment, are discussed later in this report.

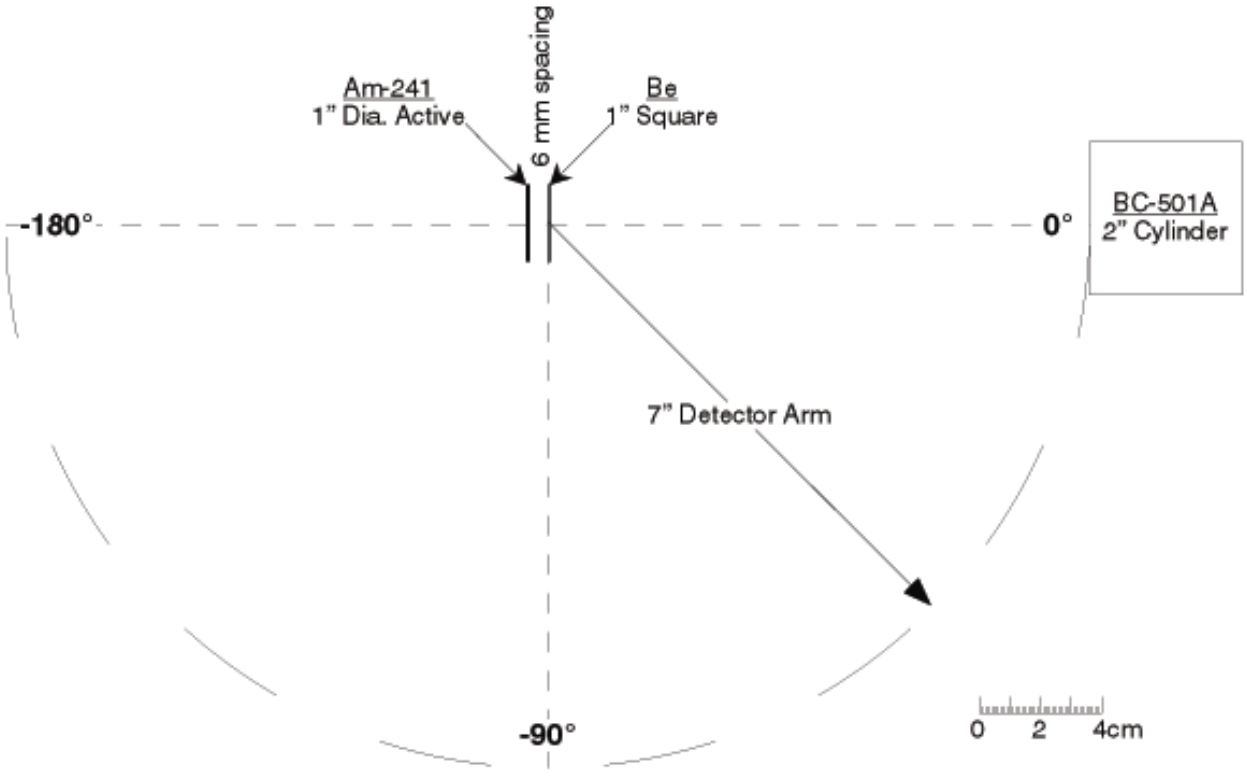

Figure 4-1. Diagrammatic view of the experimental arrangement used in the Am- Be experiment. The activity of the ^{241}Am source was 1.2 mCi, and- according to the manufacturer (Isotope Products, Burbank, CA)- the alpha emitting activity was very uniform across the 1 in. diameter active area (5.1 cm^2) of the source.

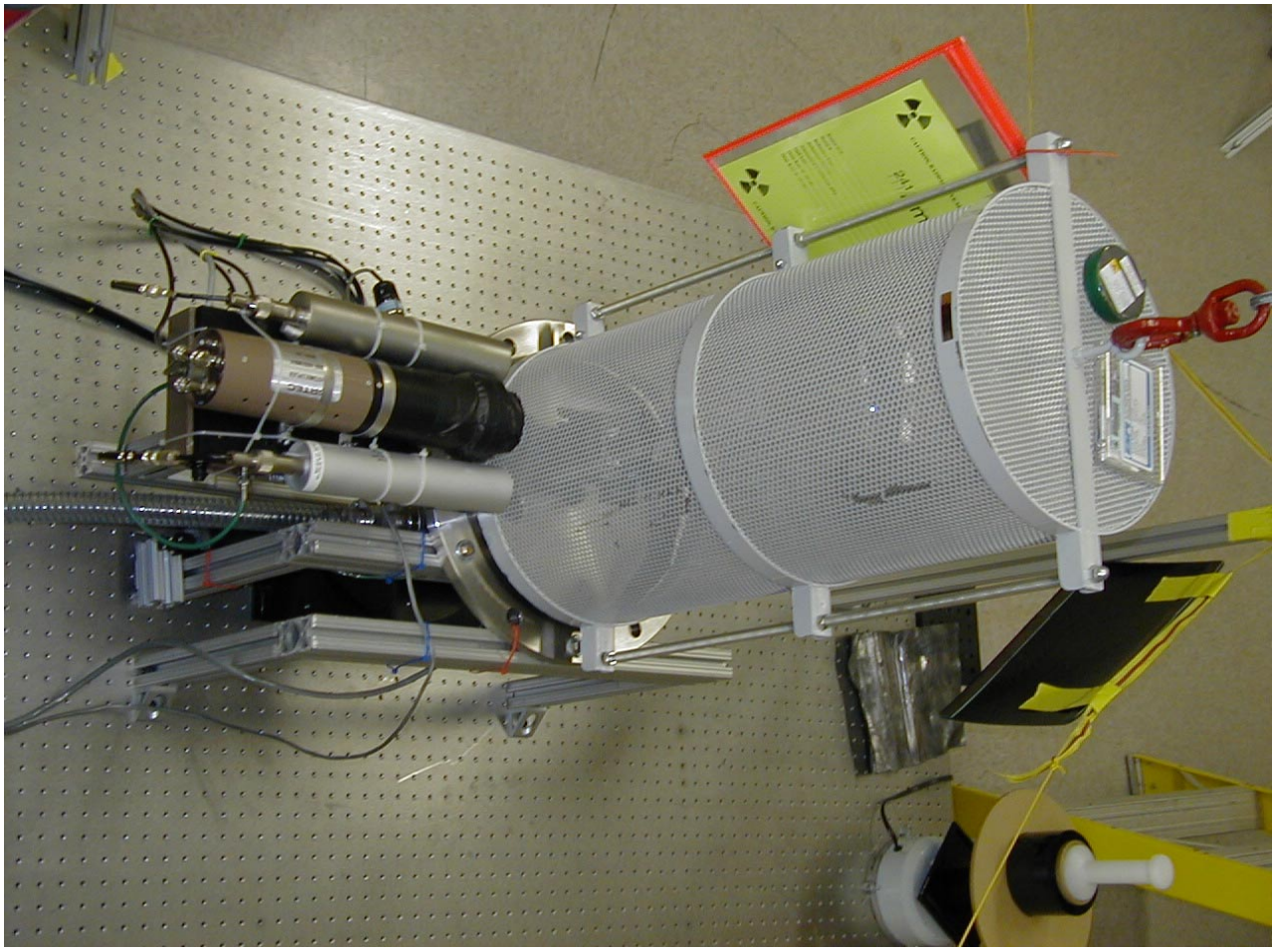

Figure 4-2. Photograph of the experimental apparatus used to measure the angular distribution of neutrons emitted from the ^{241}Am –Be neutron generator. The white cylindrical object is a metal covering for the vacuum bell jar. The neutron detectors are visible in the lower part of the photograph; the central detector with the black and brown ends is the liquid scintillator detector. The two metallic cylinders on either side of the scintillation detector are the ^{3}He and BF_3 gas detectors.

Actinium-225 - Beryllium

The ^{225}Ac-Be experiment was conceptually similar to the Am-Be experiment but the execution of the experiment involved many more steps to satisfy safety requirements. The source we used in the Ac-Be experiment was a 10 mCi ^{225}Ac source obtained from Oak Ridge National Laboratory. The 10 day half-life of ^{225}Ac insured high specific activity from the source and also enabled us to let the source "cool" after use to prevent any future disposal problems.

Long before the ^{225}Ac was delivered to SNL/CA we began designing and building the experimental apparatus for the Ac-Be experiment. Because of the higher activity and higher average energy of the alpha particles produced, we anticipated a much larger neutron production rate from Ac-Be experiment than was obtained in the Am-Be experiment. To ensure safety, a careful analysis of shielding requirements was performed as part of the experimental design. A series of computer simulations were performed with MCNP4B (LANL's general purpose Monte Carlo neutron-gamma transport code) to estimate the human dose equivalent due to neutrons, direct gamma-rays from the ^{225}Ac source, and neutron-induced gamma-rays. After several iterations we arrived at a shield design that provided ample safety margins but allowed us to run the experiment relatively unimpeded. The resulting shield design consisted of a series of 7-foot-tall, 8-inch-thick shielding panels surrounding a standard 4 ft. x 8 ft. optical table. The shield panels were filled with Poly/Cast No. 259, a castable, borated-polyethylene neutron shield material manufactured by Reactor Experiments, Inc. of San Jose, CA. The exterior of the shielding panels was composed of 1/8 inch aluminum sheets and the panels were held together with cast iron framework. Photographs of the neutron shield are shown in **Figure 4-3** and **4-4**.

The Ac-Be experiment was nearly identical to the Am-Be experiment discussed earlier, differing principally in the source target configuration. The 10 mCi ^{225}Ac source was evaporated onto a circular 1.3 cm^2 source holder by ORNL. The Be target was also circular and 1.3 cm^2 in area and was held 3.2 mm from the surface of the Ac source. Because the Be target was held so close to the ^{225}Ac source, and to mitigate safety concerns, the Ac-Be was not performed in a vacuum chamber (by contrast, the Am-Be experiment was performed in a vacuum).

As with the previous Am-Be experiment, our original intention was to monitor the output of the Ac-Be experiment with three neutron detectors; the liquid scintillator detector used in the Am-Be experiment and the two commercial gas filled detectors which previously had not functioned. Unfortunately, however, a main power interruption destroyed the PMT in the liquid scintillation detector and it was unavailable for use during the Ac-Be experiment. Instead, the two gas detectors were reconfigured after the Am-Be experiment and became fully operational; these two gas detectors were used exclusively for the Ac-Be experiment.

It is unfortunate that our detector difficulties prevented us from using the same detectors in both the Ac-Be and Am-Be experiments. The response of the two types of detectors (gas and liquid scintillator) was quite different and the results of the experiment would have been more robust if all detectors had been operational for both experiments.

Both gas detectors used in the Ac-Be experiment were manufactured by LND, Inc. of Oceanside, NY. One of the gas detectors was a ^{3}He filled type (LND #253). The ^{3}He neutron detector was cylindrical, 2.0 inches in diameter and 11.6 in. long, and it was filled to a pressure of 3040 Torr. The second gas-filled detector was an LND #2032, filled with ^{10}B-enriched BF_3, the detector was 2" in diameter and 12" in length, and was filled to 400 Torr pressure.

Two Ac-Be experiments were run in succession. In the first experiment our computer moved the two neutron detectors to 10 positions in 20 degree increments from 180 to 0 degrees. The computer stopped the detector at each step and acquired neutron count data for 6.0 hours at each angle increment. The second Ac-Be experiment was run for 19 angular steps 10 degrees apart (from 180 to 0 degrees), data was acquired for one hour at each angular increment.

Figure 4-3. Photographs of the initial assembly of the shield arrangement used for the ^{225}Ac experiment. The upper photograph shows one panel of the borated polyethylene shield (in its aluminum case) being placed in its position adjacent to the optical table. The lower photograph shows three panels of the borated shield around the optical table, as well as the cast-iron framework to support the shields.

Figure 4-4. Photograph of the completed shield assembly used for the ^{225}Ac experiment. In the upper photograph, the braced structure with warning sign attached is the door to the experimental chamber. Also visible in the photograph are the computer workstation and NIM and CAMAC electronic assemblies used to control the experiment.
In the lower photograph, a worker is shown configuring the detector assembly for the ^{225}Ac experiment. The cast iron angle bracing that supports the neutron shield is also clearly visible in this photograph.

Analysis of Experimental Results

The ^{241}Am and ^{225}Ac experiments described above, resulted in relatively simple output (a recording of the neutron count rate as a function of angle). Of course, the central question remained: was the data consistent with our prediction of a solid state neutron generator?

To answer this question we first have to return to our computer predictions and see how they can be manipulated to represent the data measured in the laboratory.

Recall that the output of the our simulation code for alpha particle transport in a SSNG resulted in an output that described the distribution of alpha particles as a function of alpha particle energy, emission angle and position. Since the experiments we performed were very large (compared to the length scale of the alpha-emitter and beryllium absorber), we need only consider the far-field solutions produced by the computer simulations. In other words, we need not consider the position dependence (across the generator) of our computer solutions as this dependence is negligible at our neutron detector position. Under the far-field assumption, we can represent the output (intensity distribution) of the alpha transport code as a function of two variables

$$\text{Alpha particle intensity} = \Psi^{\alpha}(\phi_{\alpha}, E_{\alpha}) \tag{4.1}$$

where E_{α} is the energy of the alpha particle and ϕ_{α} is the polar angle in spherical coordinates (because we expect, in the far-field assumption, that alpha particle and neutron emission are constant in the other spherical coordinate angle, θ, we will not even consider the other angle in our analysis).

In a similar fashion, we can represent the neutron output from a beryllium absorber as

$$\text{Neutron output from Be} = \Phi^{n}(\phi_{\alpha}, E_{\alpha}, \phi_{n}, E_{n}) \tag{4.2}$$

where E_n is the energy and ϕ_n the angle of the emitted neutron.

It is important to note that the neutron output defined in eq. (4.2) differs from the distributions discussed in the previous section of this report. In particular, the neutron emission distributions discussed in the last section were "thin target" distributions, i.e.; they were the angular and energy distribution of neutrons produced when a mono-energetic beam of alpha particles impinges on a thin (relative to the alpha-particle range) target of beryllium. In the laboratory, of course, our beam of alpha particles strikes a thick target of beryllium. In fact, our beryllium target is so thick (3 mm) that it is larger than the range of any alpha particle we expect to observe in our experiment. In order to construct the thick target neutron distributions from the thin target distributions given in the previous section, we first note that the alpha particle transport in the beryllium can be approximated by a continuously slowing beam that does not reduce in intensity as it slows. The "slowing down with no attenuation approximation" is probably good to the 1% level, as the removal processes (large angle scattering and reactions with the Be nuclei) occur with frequencies much lower than 1% of the alpha particle beam intensity. Under this set of assumptions, we can write an expression for the thick target neutron distribution of eq. (4.2) in terms of the thin target distribution used in Section 3

$$\Phi^n(\phi_\alpha, E_\alpha, \phi_n, E_n) = \frac{\int_0^{E_\alpha} Y(E'_\alpha)\Phi^n_{thin}(\phi_\alpha, E'_\alpha, \phi_n, E_n)dE'_\alpha}{\int_0^{E_\alpha} Y(E'_\alpha)dE'_\alpha} \quad (4.3)$$

where $Y(E_\alpha)$ is the efficiency for producing neutrons of a given alpha energy in a thick target (see equation (2.1). The integral in the denominator is used to normalize $\Phi^n(\phi_\alpha, E_\alpha, \phi_n, E_n)$, since $Y(E_\alpha)$ itself is not normalized.

With the thick target correction and re-normalization of the neutron output complete, we can now predict the neutron distribution in the laboratory. The neutron output of the generator we measure in the lab should be given by the two-dimensional convolution of alpha intensity of the generator with the thick target neutron output

$$\Phi^{n,predicted}(\phi_n, E_n) = \iint \Phi^n(\phi_\alpha - \phi'_\alpha, E_\alpha - E'_\alpha, \phi_n, E_n)\Psi^\alpha(\phi'_\alpha, E'_\alpha)Y(E'_\alpha)dE'_\alpha d\phi'_\alpha \quad (4.4)$$

Because these calculations were performed numerically on the computer, we used discrete approximations to the continuous functions, replaced the integrals with summations, and the answers were in the form of multidimensional matrices. A visualization of the calculations performed to simulate the Am-Be experiment is shown in **Figures 4-5** and **4-6**. Both the thick target output for normally incident 5.5 MeV alpha particles from ^{241}Am, $\Phi^n(\phi_\alpha = 0^o, E_\alpha = 5.5MeV, \phi_n, E_n)$, and the estimated output of the neutron generator $\Phi^{n,predicted}(\phi_n, E_n)_{Am-Be}$ obtained by convolving the angular distribution of incoming alphas with the neutron generator output are shown in the figures.

The results of a similar calculation for the Ac-Be experiment is shown in **Figure 4-7**; here only the convolved, final result, $\Phi^{n,predicted}(\phi_n, E_n)_{Ac-Be}$ is shown for clarity.

Unfortunately, our neutron detection apparatus was not capable of measuring the neutron energy distribution, instead only a single count rate as a function of angle was measured. To predict the detector count output as a function of angle we must integrate the neutron energies over the neutron detector response function, $\eta(E_n)$

$$N(\phi_n) = \int \Phi^{n,predicted}(\phi_n, E'_n)\eta(E'_n)dE' \quad (4.5)$$

Like most neutron detectors, the ones we used in this experiment were not calibrated for efficiency at all neutron energies. Furthermore, the angular response of our detector was not known. Our experiment was configured in such a way that the neutrons arrived at the detector always normal to the face of the detector; thus, under these conditions, we can eliminate the angular dependence of the detector response function. Our simple estimate of the detector response function was

$$\eta(E_n) = 1 - e^{-\sigma(E_n)\rho d} \quad (0.1)$$

where $\sigma(E_n)$ is the neutron interaction cross-section for the interaction that led to a count inside the detector, ρ is the number density of the interacting species in the detector and d is the detector thickness. Widely accepted cross-sections (ENDF) were used in our

detector response calculations, and together with information provided by the manufacturer of the detector, we estimated the response as a function of energy for all three detectors used in the study. The results of these calculations are shown in **Figure 4-8**.

The final comparison of theory with experiment was made by performing the computation of eq. (4.5) and using the appropriate detector response function given by eq.(4.6). The results of these calculations are shown in **Figure 4-9** for the Am-Be experiment and in **Figures 4-10** and **4-11** for the two runs of the Ac-Be experiment.

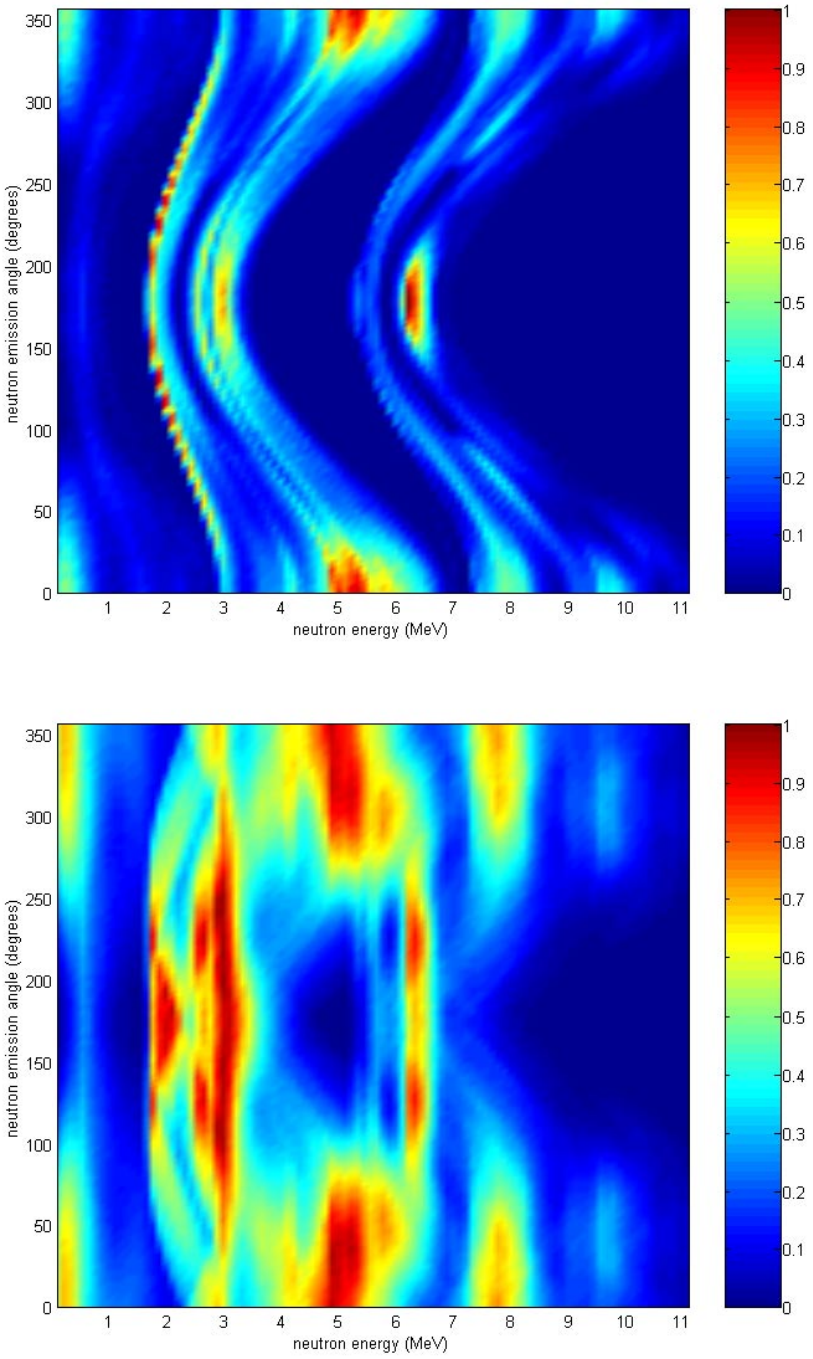

Figure 4-5. Visualization of the neutron energy distribution expected from 5.5 MeV alpha particles impinging on a thick beryllium target. The upper plot illustrates the expected neutron emission distribution, $\Phi^n(\phi_\alpha = 0^o, E_\alpha = 5.5MeV, \phi_n, E_n)$, for a beam of alpha particles normally incident on a beryllium target. The lower plot illustrates the expected neutron distribution from the ^{241}Am experiment, $\Phi^{n,predicted}(\phi_n, E_n)_{Am-Be}$, obtained by convolving the distribution in the upper plot with the estimated angular distribution of alpha particles expected in our experiment.

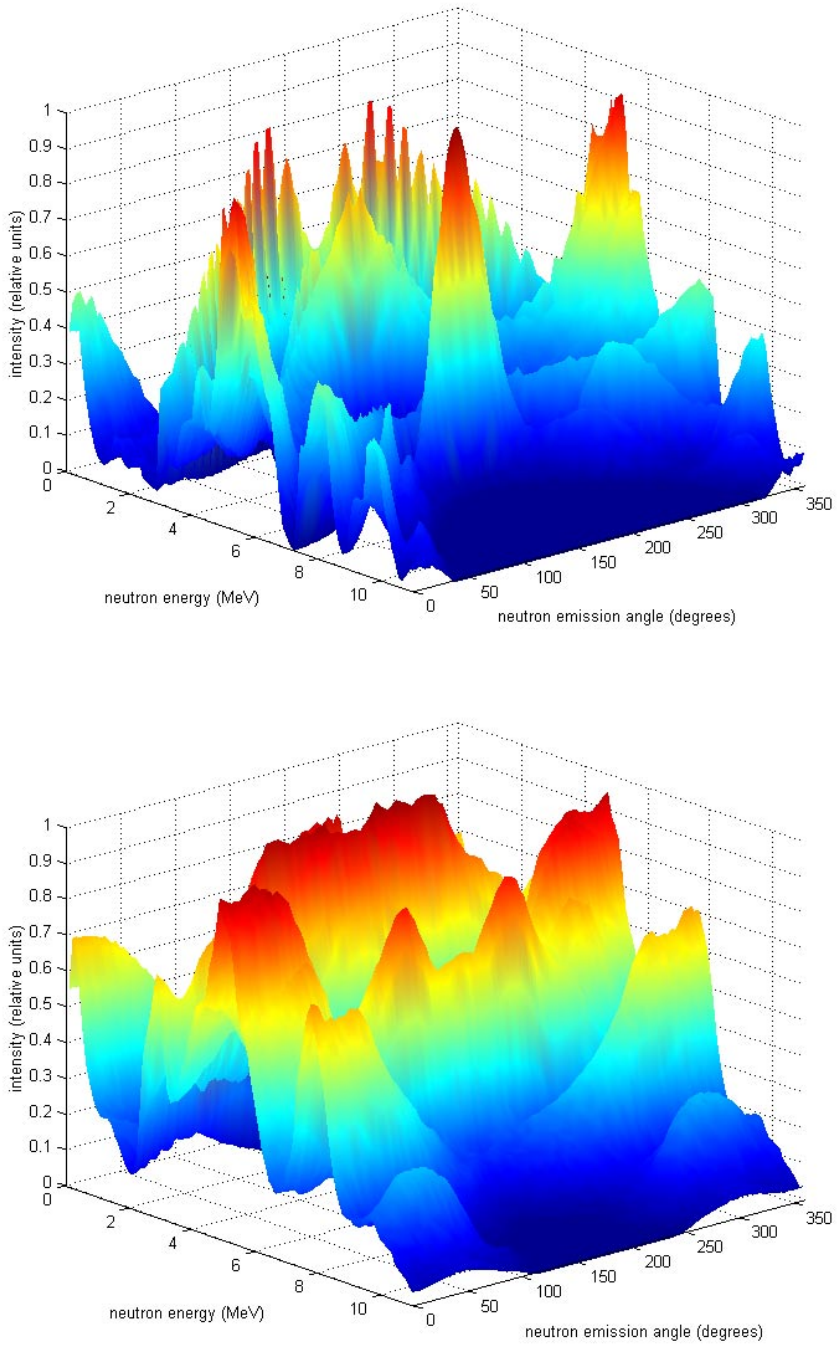

Figure 4-6. Another visualization of the neutron energy distribution expected from the Am-Be experiment. The upper plot illustrates the expected neutron emission distribution, $\Phi^n(\phi_\alpha = 0^o, E_\alpha = 5.5MeV, \phi_n, E_n)$, for a beam of alpha particles normally incident on a beryllium target. The lower plot illustrates the expected neutron distribution from the ^{241}Am-Be experiment, $\Phi^{n,predicted}(\phi_n, E_n)_{Am-Be}$, obtained by convolving the distribution in the upper plot with the estimated angular distribution of alpha particles expected in our experiment.

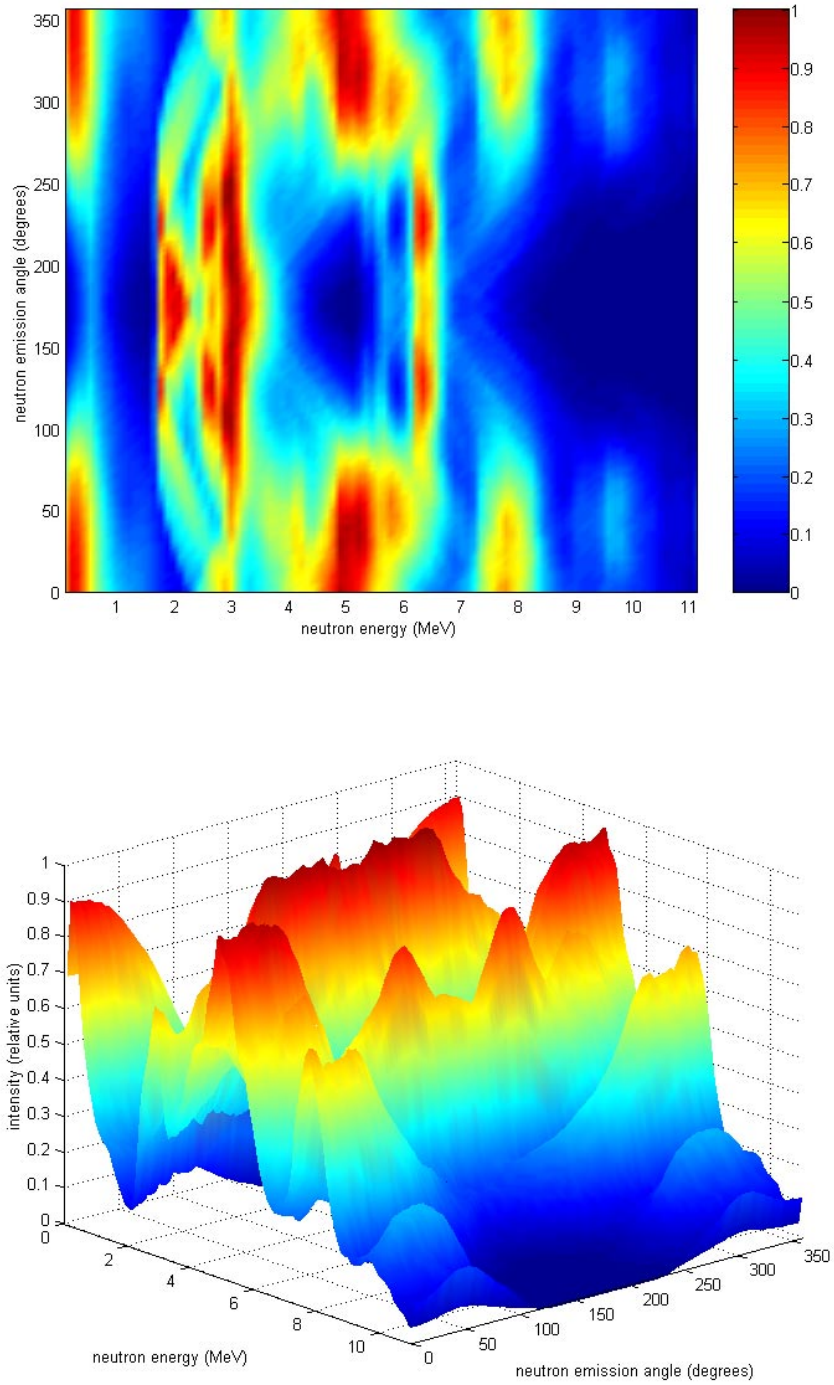

Figure 4-7. Two visualizations of the expected results from the ^{225}Ac experiment. Both plots depict the expected neutron emission intensity as a function of neutron emission angle and neutron energy, $\Phi^{n,predicted}(\phi_n, E_n)_{Ac-Be}$. Note the difference in the distribution from the results expected from the ^{241}Am experiment and shown in **Figures 4-5** and **4-6**.

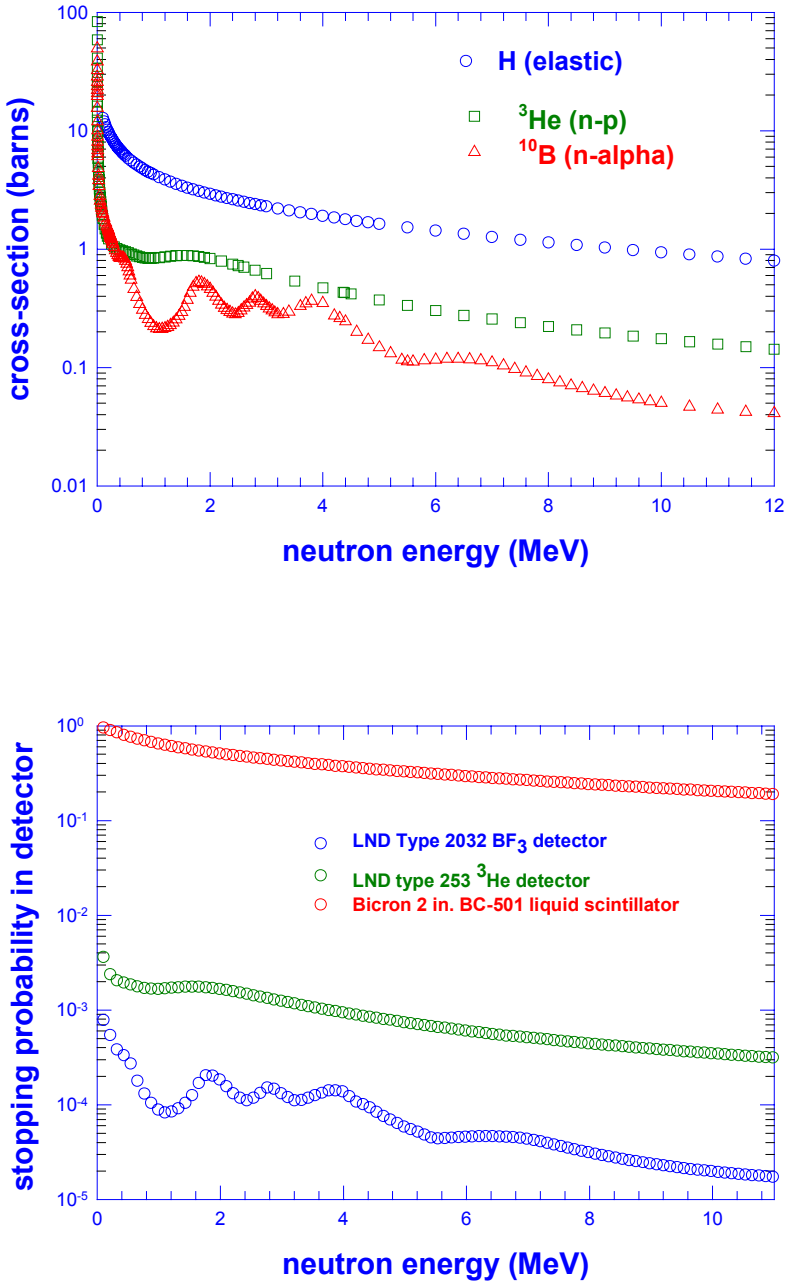

Figure 4-8. Upper plot: neutron cross-section as a function of energy for nuclear reactions occurring in the neutron detectors used in the experiments. Lower plot: estimated efficiency of detectors used to record the emission signal in our experiments. The plots in the lower figure are a depiction of the detector response function, $\eta(E_n) = 1 - e^{-\sigma(E_n)\rho d}$, used in our calculations.

The agreement between the theoretical predictions and the experimental results was very good for the Am-Be experiment, but less good for the Ac-Be experiments. The confirmation of the non-isotropic output of the Am-Be and the good agreement between theory and experiment for that experiment (both theory and experiment show an angular isotropy of approximately a factor of two) stand as confirmation of the theoretical basis used in our calculations. More importantly, the results of the Am-Be experiment provide an absolute confirmation that solid state neutron generators with highly anisotropic output are feasible.

The difference between theory and experiment was much wider for the Ac-Be experiments and there could be a number of reasons for the discrepancy. Perhaps the most reasonable explanation for the discrepancy is related to the detector response. In the Ac-Be experiments only the ^{3}He and BF_3 detectors were functional. Both of these detectors rely on "1/v" neutron cross-section interaction processes; thus these detectors are much more sensitive to very low energy neutrons than the scintillation detector used in the Am-Be experiment. It is quite possible that neutrons would scatter off of the large hydrogenous neutron shield present around the Ac-Be experiment and back into the detectors. This effect would suppress the angular dependence of the neutron output as recorded by the detectors. Another possible reason for the difference between theory and experiment for the Ac-Be experiment is the computation error. A very large number of steps went into the Ac-Be particle transport simulation and it is much more likely for an error to have occurred in the Ac-Be computation than with the simpler, essentially mono-energetic Am-Be computation. Possible computation errors could have resulted in coding errors on our part or from a possible erroneous cross-section or branching ratio used in the calculation.

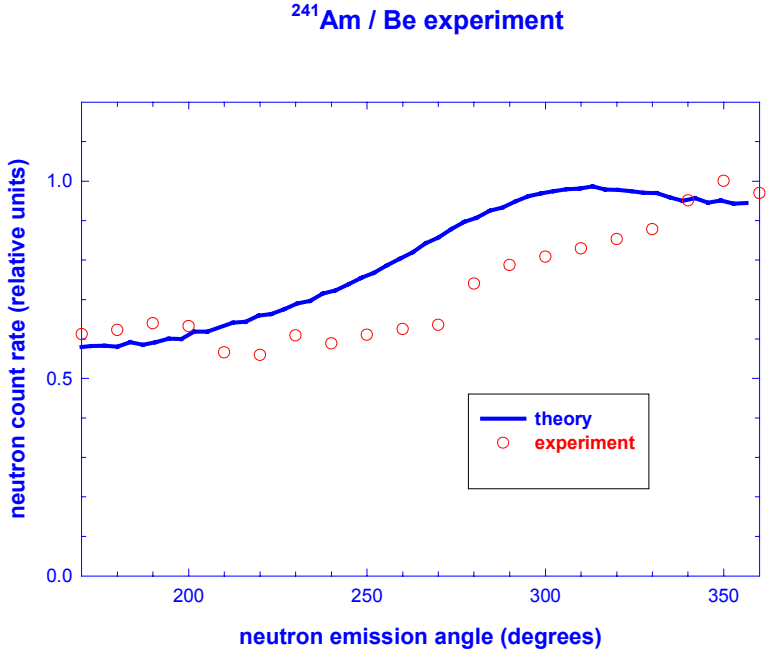

Figure 4-9. Comparison of the experimental results (obtained with a 2 in. liquid scintillator detector) and the theoretical prediction (based on using the transport code described in the text, and folding in the detector response). Considering the experimental and theoretical uncertainties, the agreement is quite good.

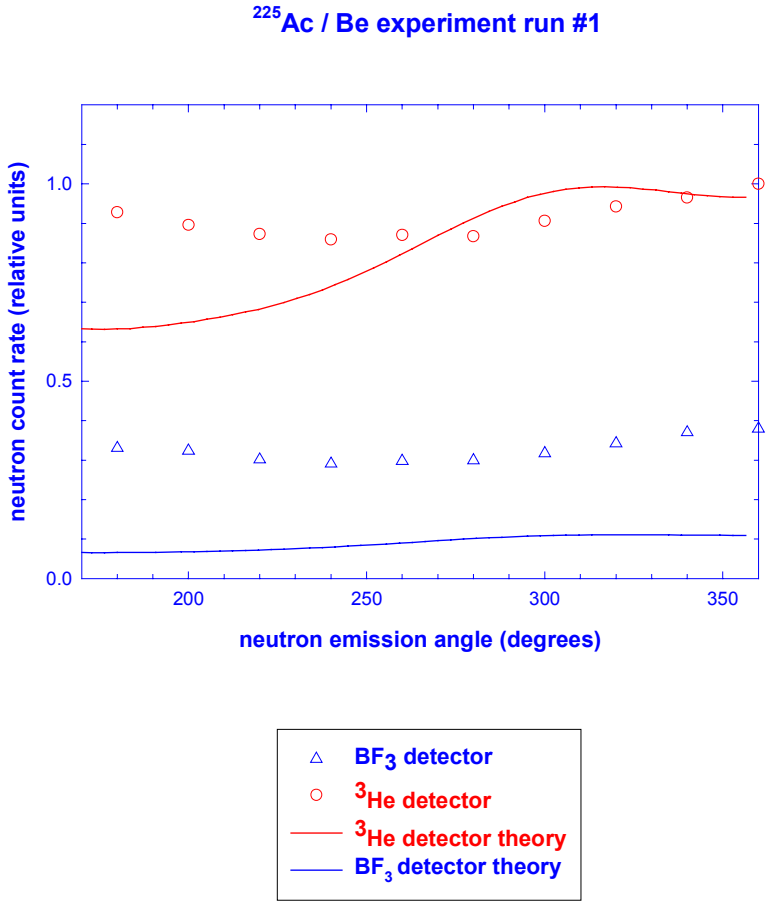

Figure 4-10. Comparison of the experimental results and the theoretical prediction for the first run of the ^{225}Ac-Be experiment. Experimental results are shown as discrete symbols and the theoretical predictions are shown as continuous solid lines. The blue lines and symbols represent the prediction and measured results for the BF_3 detector (LND, Inc. #2032) and the red lines and symbols represent the prediction and results (respectively) for the ^{3}He Detector (LND, Inc. #253). Agreement between prediction and experimental results is less than in the Am-Be experiment. The relatively wide disparity between predicted and measured results may be due to several reasons, including: interference from low energy neutrons scattering from the borated polyethylene shield, and errors in the calculations used in the prediction.

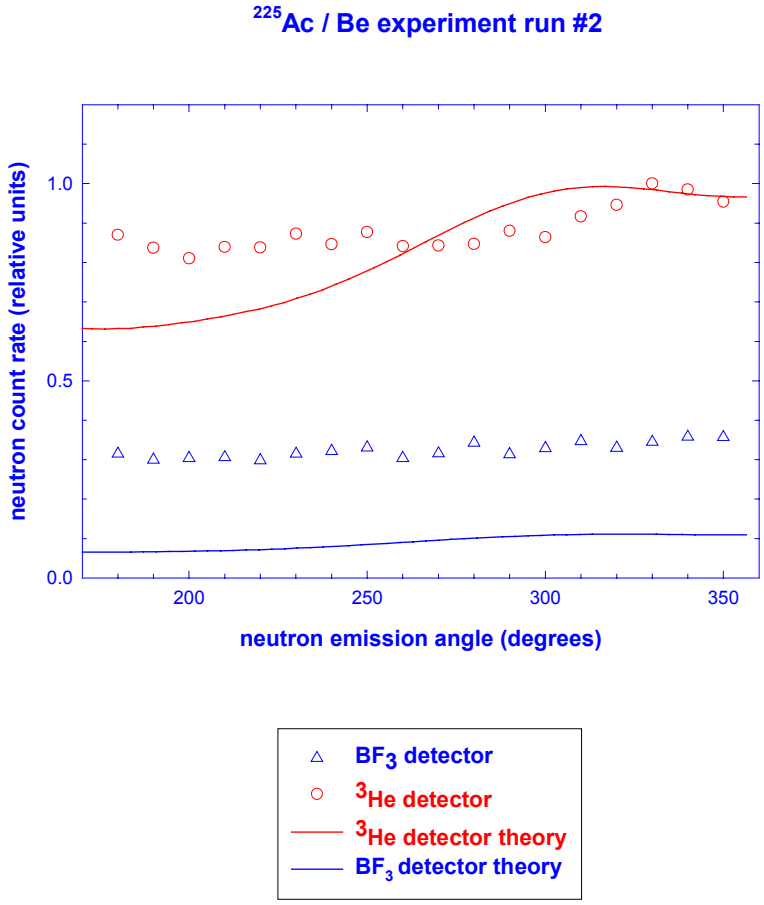

Figure 4-11. Comparison of the experimental results and the theoretical prediction for the second run of the ^{225}Ac-Be experiment. Experimental results are shown as discrete symbols and the theoretical predictions are shown as continuous solid lines. The blue lines and symbols represent the prediction and measured results for the BF_3 detector (LND, Inc. #2032) and the red lines and symbols represent the prediction and results (respectively) for the ^{3}He Detector (LND, Inc. #253). Agreement between prediction and experimental results is less than in the Am-Be experiment, but better than in the first Ac-Be run.

Demonstration of Fabrication Technologies

Our demonstration through computer simulation and later through experiment showed clearly that micro-machined solid state neutron generators are feasible and would have interesting properties (notably the anisotropic neutron emission). What was equally important to demonstrate in our research project was that parts could be fabricated with the requisite properties for use in micro-fabricated neutron sources.

Our investigation into fabrication technologies was divided into two areas, an examination of motion control devices for moving the small alpha particle barriers, and-

more importantly- an investigations into fabrication processes for making suitable alpha particle barriers.

Our investigation of motion control devices involved an examination of commercially available "micro translators" and their applicability to SSNGs. We found that there were a variety of commercially available devices that would be suitable in this application. The two most suitable motion control technologies that we found were miniaturized forms of classical electromagnetic translators (motors and solenoids) and piezo-electric transduction devices. A demonstration unit was fabricated from a simple electromagnetic rotary solenoid actuating a beryllium shutter. Photographs of this demonstration unit are shown in **Figure 4-12**. This demonstration unit actually comprised a working switchable solid state neutron generator. However, the output of the generator was barely measurable due to the very low intensity of the ^{241}Am source used in the unit (10 μCi).

Our investigation of micro-manufacturing techniques to produce parts for solid state generators was vigorous and successful. We were eventually able to demonstrate fabrication processes that produced parts with nearly ideal specifications for use in micro-SSNGs. **Figures 4-13** and **4-14** outline manufacturing processes for producing alpha particle blocking layers for the "pumpkin teeth" generator topology. **Figures 4-15** and **4-16** show photographs of parts that were fabricated from gold using these processes.

Summary of Experimental Results

Two large-scale experiments were performed that confirmed the operation of solid state neutron generators. One experiment used a simple configuration of a nearly mono-energetic alpha emitting source- ^{241}Am- and the other used a much more complicated short-lived alpha particle emitter- ^{225}Ac. Agreement between theory and experiment was quite good for the first experiment and less so for the Ac-Be experiment. The fabrication experiments were quite successful; we demonstrated that it was possible to build parts of the correct dimensions to function in micro-machined, solid state neutron generators.

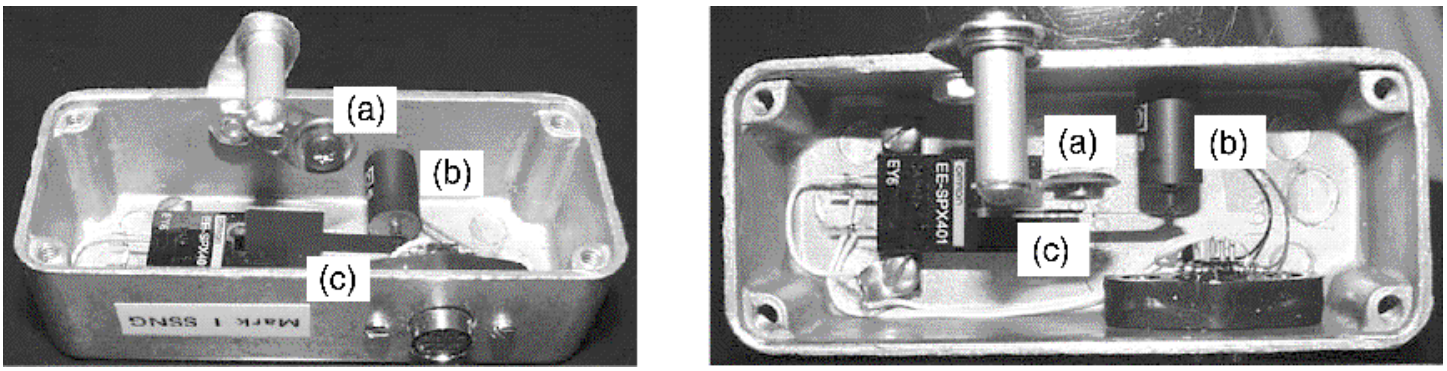

Figure 4-12. Photograph of a simple prototype solid state neutron generator. Referring to the labels in the photograph: (a) indicates the ^{241}Am alpha emitting source, (b) is a small rotary solenoid used to rotate the beryllium plate (c) in front of the alpha source. The generator is shown in the "off" state (beryllium plate away from source). When activated, the rotary solenoid places the beryllium source in close proximity to the ^{241}Am alpha particle source.

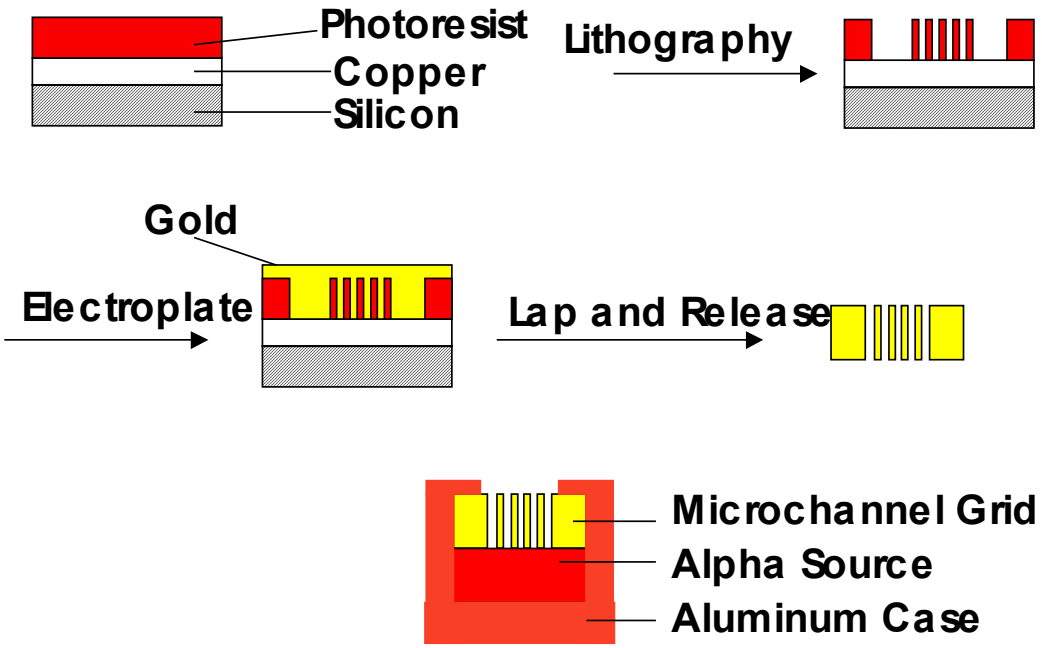

Figure 4-13. Diagrammatic illustration of the steps used to fabricate the micro-machined parts for use in a solid state neutron generator. The diagram illustrates the process steps used to fabricate the alpha particle source and its micro-channel gold plate used in the "pumpkin teeth" design.

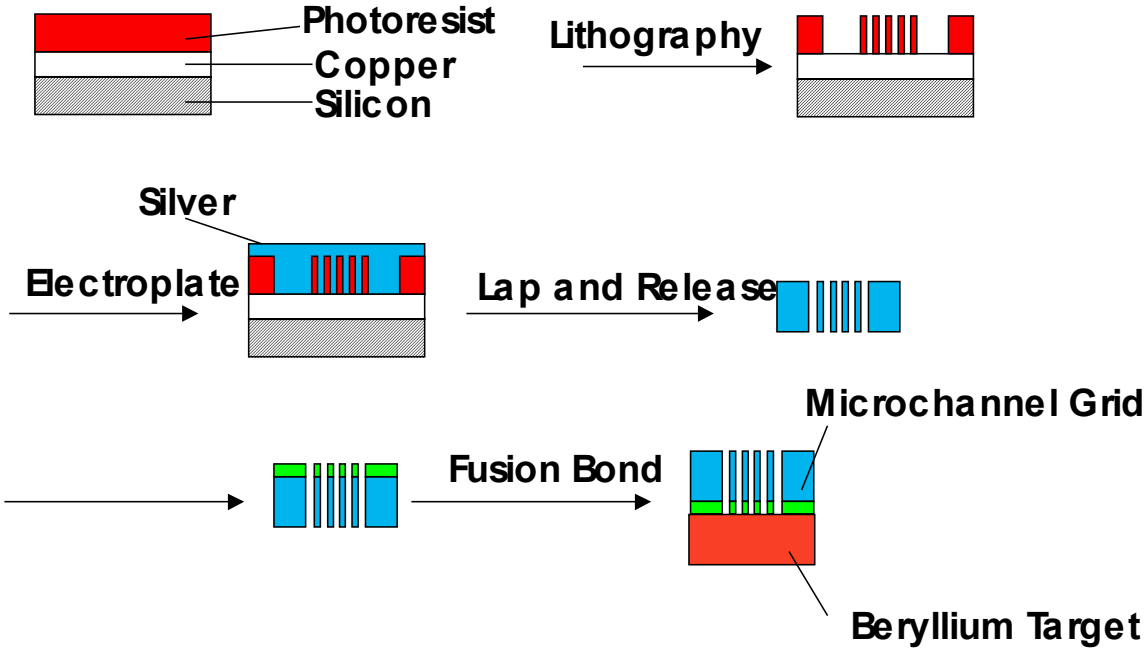

Figure 4-14. Diagrammatic illustration of the steps used to fabricate the beryllium target assembly for use in a "pumpkin teeth" design solid state neutron generator.

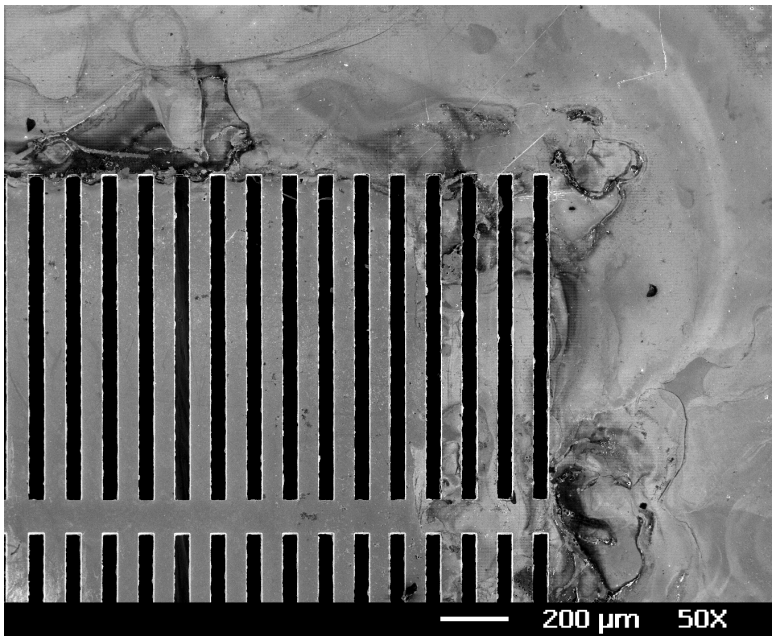

Figure 4-15. Scanning electron micrograph of a micro-channel gold plate fabricated using the process outlined in **Figure 4-13**. The long slots in the electroplated gold foil are 1000 µm long and 50 µm wide. The gold between the slots is 60 µm wide and the gold support ribs (at right angles to the slots) are 100 µm wide. The black discoloration is a residue from the plating operation used to produce the gold foil.

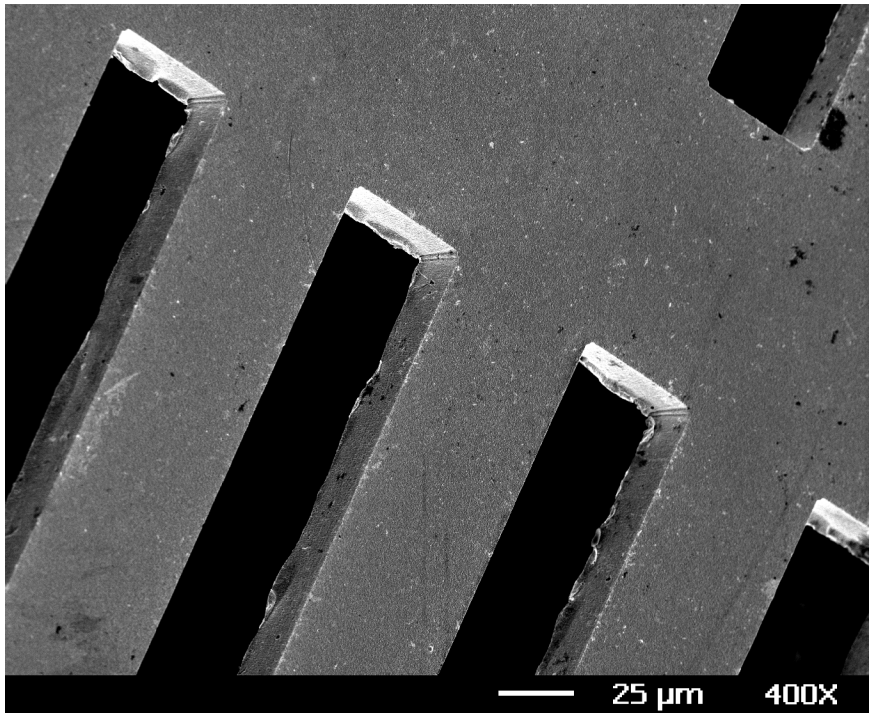

Figure 4-16. Scanning electron micrograph of a micro-channel gold plate. This photograph is taken at higher magnification than **Figure 4-15** and reveals the structure of the apertures in the 20 µm thick electroplated gold foil.

APPENDIX A—References

1) F. Ajzenberg-Selove, P.H. Stelson, 1960, “Be9(a,n)C12 Reaction and the Parameters of the 7.66-MeV State of C12”, *Physical Review,* vol.120, no. 2, pp. 500-504.

2) F. Ajzenberg-Selove, T. Lauritsen, 1968, “Energy Levels of Light Nuclei (VII) A=11-12”, *Nuclear Physics,* vol. A114, pp. 1-142.

3) ANSI, 1991.

4) J.K. Bair, J. Gomez del Campo, 1979, “Neutron Yields from Alpha-Particle Bombardment”, *Nuclear Science and Engineering,* vol. 71, pp. 18-28.

5) T.W. Bonner, Alfred A. Kraus J.R., J.B. Marion, J.P. Schiffer, 1956, Neutrons and Gamma-rays From The Alpha-Particle Bombardment of Be9, B10, B11, C13, and O18, *Physical Review*, vol. 102, no. 5, pp. 1348-1354.

6) D.L. Bowers, E.A. Rhodes, L.E. Dickerman, 1988, A Switchable Radioactive Neutron Source: Proof-of-Principle, *Journal of Radioanalytical and Nuclear Chemistry*, vol. 233, pp. 161-165.

7) H.H. Barschall, …, S. Cierjacks, …, G.G. Knoll, et al., 1983, Neutron Sources For Basic Physics and Applications, Pergamon Press, New York.

8) Klaus W. Geiger, L. Van der Zwan, H. Werle, 1973, “The Neutron Spectrum of a 227Ac-Be(a,n) Source”, *International Journal of Applied Radiation and Isotopes*, vol. 24, pp. 165-169.

9) K.W. Geiger and L. Van der Zwan, 1975, “Radioactive Neutron Source Spectra from 9Be(a,n) Cross Section Data”, *Nuclear Instruments and Methods*, vol. 131, pp. 315-321.

10) J.H. Gibbons, R.L. Macklin, 1964, “Total Cross Section for 9Be(a,n)”, *Physical Review*, vol. 137, no. 6B, pp. B1508-1509.

11) J.H. Gibbons, R.L. Macklin, 1959, “Total Neutron Yields from Light Elements Under Proton and Alpha Bombardment”, *Physical Review*, vol. 114, no. 2, pp. 571-580.

12) H.J. Hirsch, Hj. Matzke, 1972, “Stopping Power and Range of a-Particles in (u,pu) and UC and Application to Self-Diffusion Measurements Using Alpha-Spectroscopy”, *Journal of Nuclear Materials,* vol. 45, pp. 29-30.

13) G.J.H. Jacobs, H. Liskien, 1983, “Energy Spectra of Neutrons Produced By a-Particles in Thick Targets of Light Elements”, *Ann. Nucl. Energy*, vol. 10, no. 10, pp. 541-552.

14) R. B. James, 2000, private communication.

15) Lord Kelvin, John Joly, William Francis, 1905, The London, Edinburgh, and Dublin Philosophical Magazine and Journal of Science, vol. X-sixth series, pp. 317-341.

16) D.L. Lessor, R.E. Schenter, 1971, Neutron Spectra From (a,n) Reactions In Plutonium Compounds Calculated From Hauser-Research Reaction Theory.

17) R.G. Miller, R.W. Kavanagh, 1966, “The Reaction 9Be(a,n)12C”*, Nuclear Physics,* pp. 492-500.

18) A.W. Obst, T.B. Grandy, J.L. Weil, 1972, “Reaction 9Be(a,n)12C from 1.7 to 6.4 MeV”, *Physical Review C,* vol. 5, no. 3, pp. 738-754.

19) Hugh T. Richards, Lyda Speck, 1944, Energy Spectrum of Po-Be Neutrons, CIC-14 Report Collection.

20) J.R. Risser, J.E. Price, L.M. Class, 1956, “Resolved Neutrons from the Be (a,n) Reaction”, *Physical Review*, vol. 105, no. 4, pp. 1288-1293.

21) J. Pal, S. Saha, C. C. Dey, B. K. Sinha, and M. B. Chatterjee, 1998, "Neutron Energy Spectrum of Am-Be Source by Gamma Gated NTOF Technique", in *Radiation Physics and Chemistry*, vol. 51, pp. 475-477.

22) L. Van der Zwan, 1968, “Calculated Neutron Spectra from 9Be(a,n) Sources”, *Canadian Journal of Physics*, vol. 46, pp. 1527-1536.

23) B.G. Whitmore, W.B. Baker, 1950, “The Energy Spectrum of Neutrons from A Po-Be Source”, *Physical Review*, vol. 78, no. 6, pp. 799-801.

24) J.F. Ziegler, J.P. Biersack, and U. Littmark, 1985, The Stopping and Range of Ions in Solids, vol. 1, Pergamon Press, New York.

Distribution

1

Attn: G. Hux

Livermore, CA 94550

1	MS	9007	D. Henson, 8400
1		9101	C. A. Nilsen, 8411
1		9102	A. L. Hull, 8416
2		9401	A. M. Morales, 8729
2		9402	K. L. Hertz, 8724
2		9671	N. R. Hilton, 8411
5		9671	J. C. Lund, 8411
1		9671	B. A. Brunett, 8416
2		9671	J. M. Van Scyoc, 8416
1	MS	0188	D. L. Chavez, LDRD Office, 1030
3	MS	9018	Central Technical Files, 8945-1
1		0899	Technical Library, 9616
1		9021	Classification Office, 8511/Technical Library, MS 0899, 9616
1		9021	Classification Office, 8511 for DOE/OSTI